Expanding and quantifying the crystal chemistry of the flexible ligand 15aneN5

Anthony D. Shircliff,[a] Elisabeth M. A. Allbritton,[a] Dustin J. Davilla,[a] Michael-Joseph Gorbet,[a] Donald G. Jones,[a] David S. Tresp,[a] Michael B. Allen,[a] Alina Shrestha,[a] Gwendolyn E. Burgess,[a] John I. Eze,[a] Andrea T. Fernandez,[a] Daniel Ramirez,[a] Kody J. Shoff,[a] Garet G. Crispin,[a] Sarah B. Crone,[a] Michael Flinn,[a] Tien Tran,[a] Darby S. Bryce,[a] Abbagale L. Bond,[a] Dylan W. Shockey,[a] Allen G. Oliver,[c] Jeanette A. Krause,[d] Timothy J. Prior,*[b] and Timothy J. Hubin*[a]

[a] Department of Chemistry and Physics, Southwestern Oklahoma State University, 100 Campus Drive, Weatherford, OK, USA E-mail: tim.hubin@swosu.edu http://faculty.swosu.edu/tim.hubin/
[b] Department of Chemistry, University of Hull, Cottingham Road, Kingston Upon Hull, HU6 7RX, UK
[c] Department of Chemistry and Biochemistry, University of Notre Dame, Notre Dame IN, USA
[d] Department of Chemistry, University of Cincinnati, Cincinnati, OH, USA

Table of Contents

SECTION 1: CRYSTALLOGRAPHIC INFORMATION FOR LIGANDS AND INTERMEDIATES

GBMA01, intermediate 2

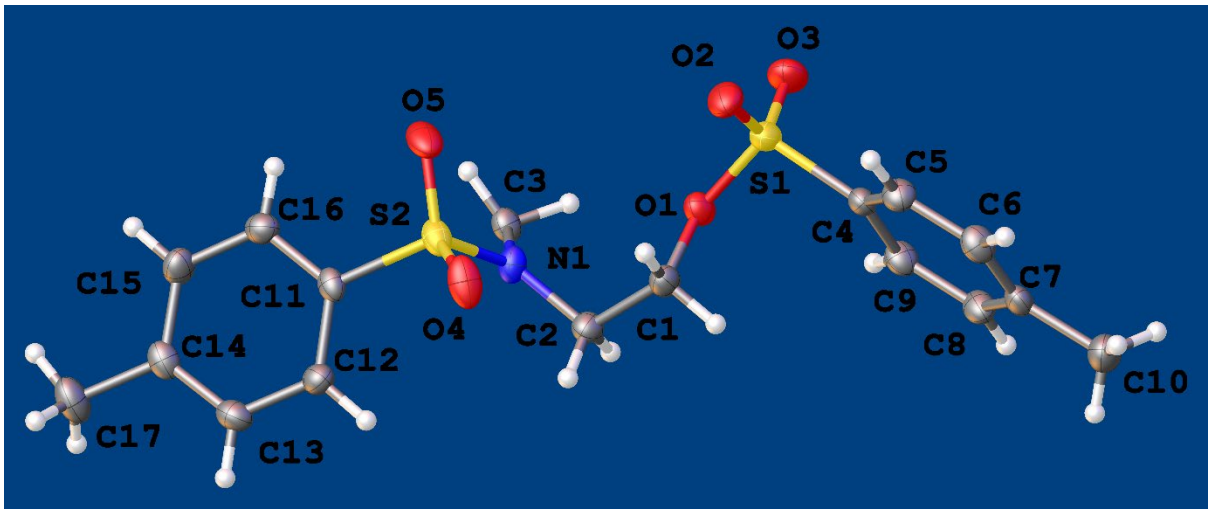

Figure L1: Asymmetric unit of GBMA01, intermediate **2**, with atoms drawn as 50 % probability ellipsoids.

The crystal examined was rather poorly-scattering and it was not possible to identify diffraction data above the noise towards the edge of the detector. The data were therefore chopped at d = 0.84 Å for refinement.

The asymmetric unit contains one half of molecule **2**. The full molecule is generated by the centre of inversion in the space group $P2_1/n$ and is shown below.

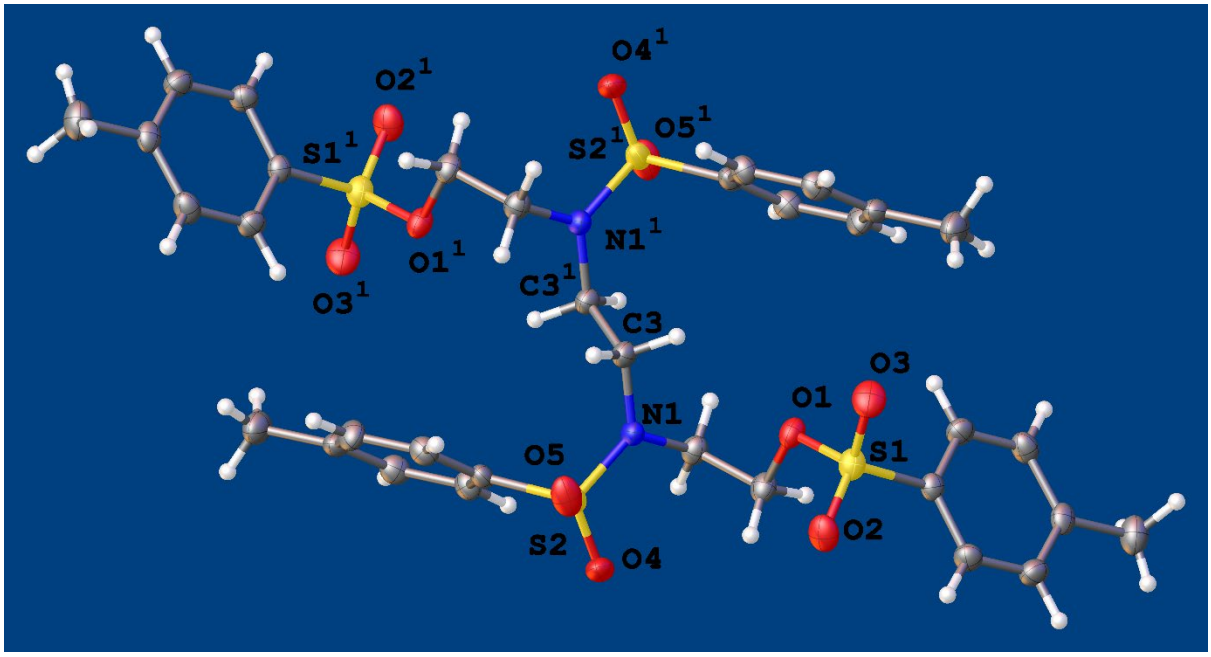

Figure L1b: Intermediate **2** in the solid state, with atoms drawn as 50 % probability ellipsoids. Symmetry operator used to generate equivalent atoms: 1 = 1–*x*, 1–*y*, 1–*z*.

There are no classical hydrogen bonds within the structure, but there are S=O···H-C (aromatic) contacts between adjacent molecules. There are further S=O···H-C (sp^2 and sp^3) contacts but it is not clear whether these should be regarded as stabilising the structure. The packing of **2** is shown below.

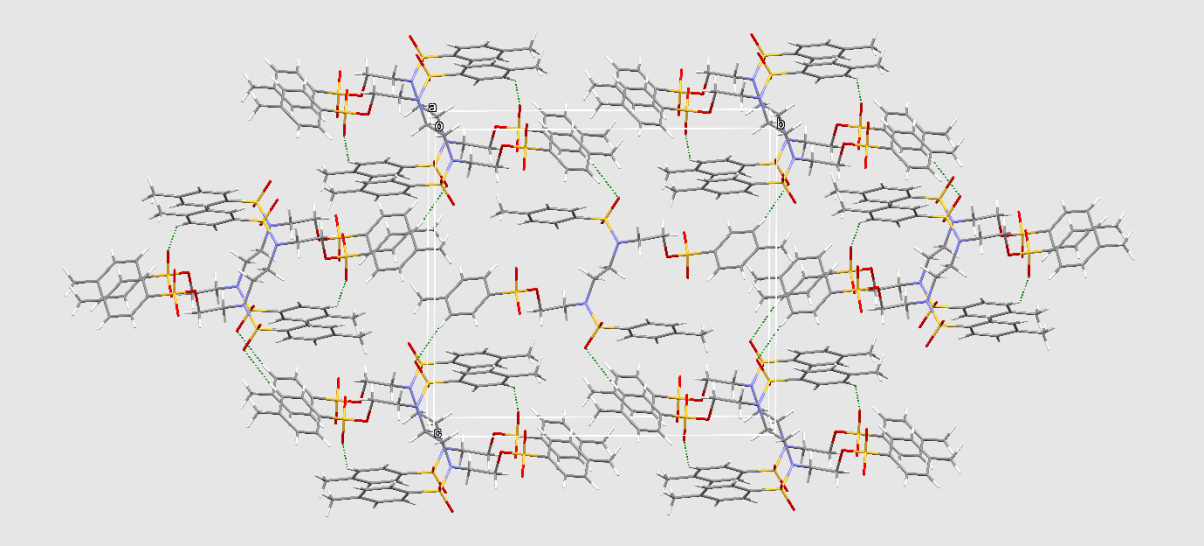

Figure L1c: Intermediate **2** in the solid state with aromatic contacts. Dashed lines show S=O···H-C (aromatic) contacts.

EMAA02C, intermediate 3

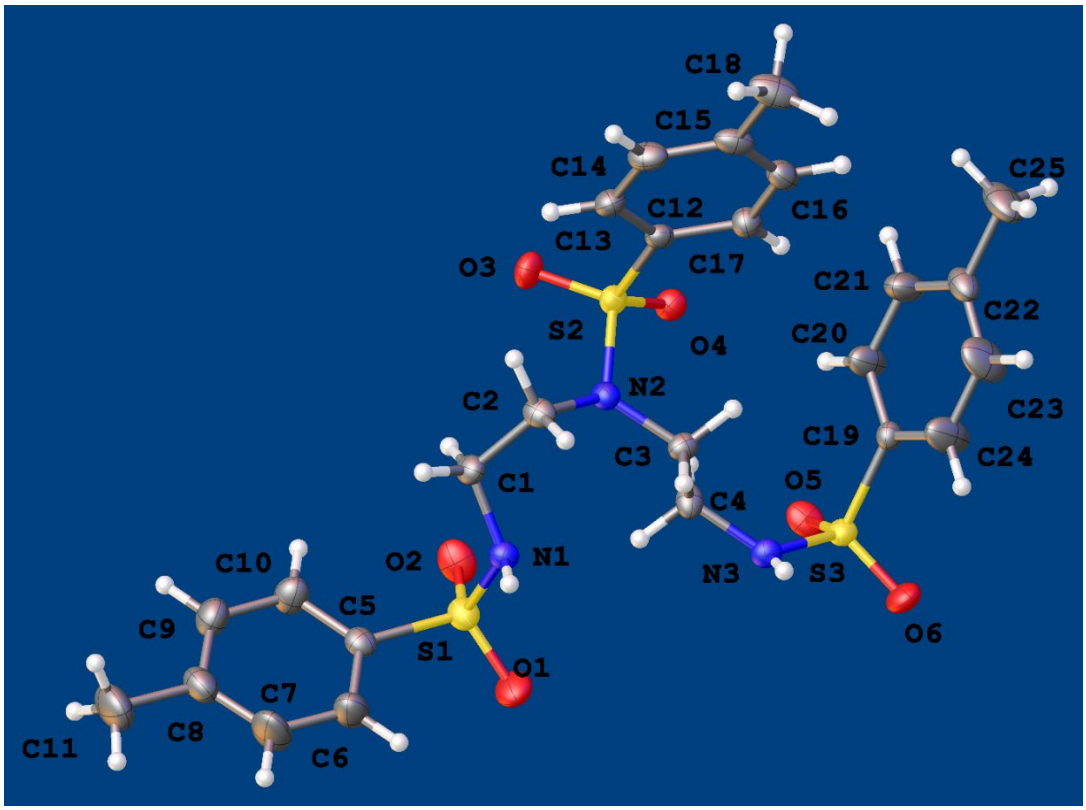

Figure L2: Asymmetric unit of EMAA02C, intermediate **3**, with atoms drawn as 50 % probability ellipsoids.

Structure solution and refinement in the centric space group $P2_1/n$ were completely routine.

In the solid state the molecules are arranged in hydrogen-bonded tapes that run parallel to the *a*-axis. There are pairs of N-H···O interactions between adjacent molecules as shown in Figure L2a.

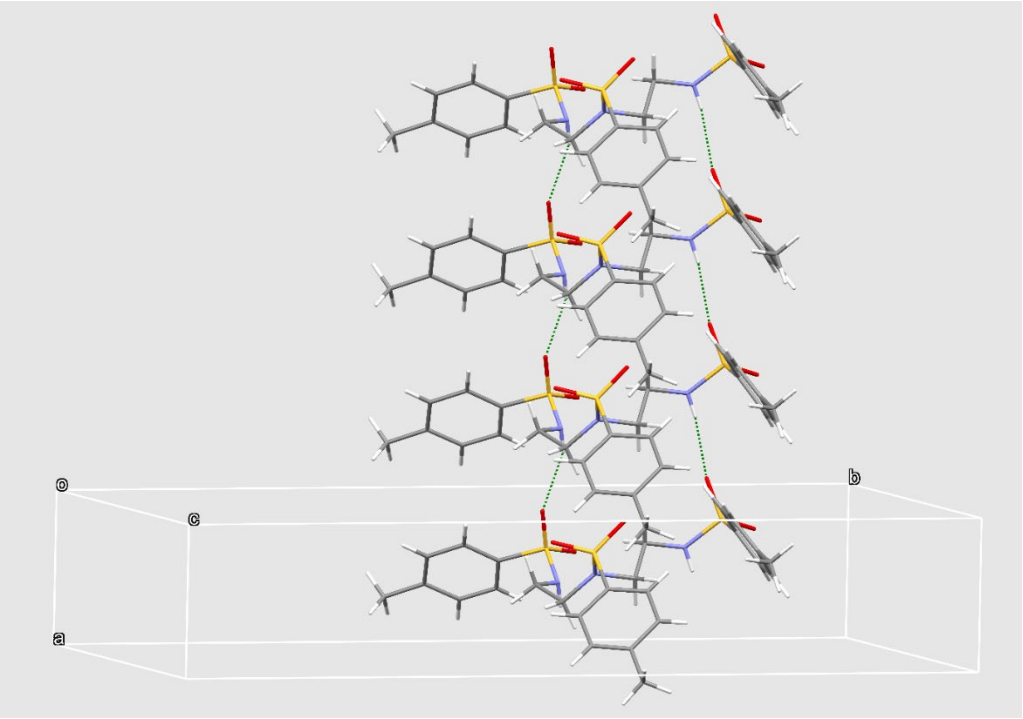

Figure L2b: Classical hydrogen bonding present in EMAA02C, intermediate **3**. Classical hydrogen bonds are shown as dashed lines.

ADS102 pure ligand Z' = 2 number 15aneN5

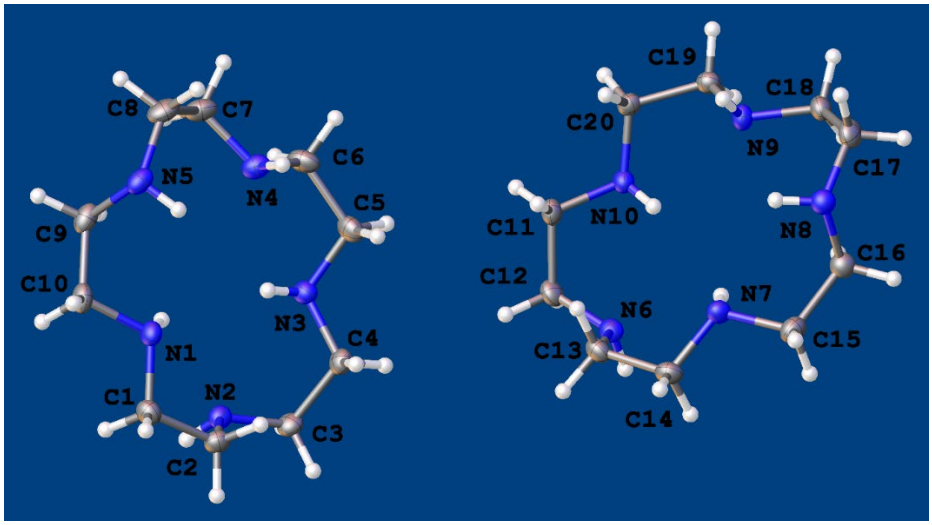

Figure L3: Asymmetric unit of ADS102, **15aneN5**, with atoms drawn as 50 % probability ellipsoids. Small-scale disorder (~8% occupied) in the second molecule is not shown.

The ligand crystallises in the centric space group P-1 with two separate molecules in the aysmmetric unit (Z' = 2). Four badly-fitted reflections were omitted from the final cycles of refinement.

In the solid, the molecules are arranged in hydrogen-bonded columns through N-H···N interactions. Identical molecules pack along *a* to form these columns. The two symmetry-unique macrocycles are not present in the same columns. This stacking is shown below.

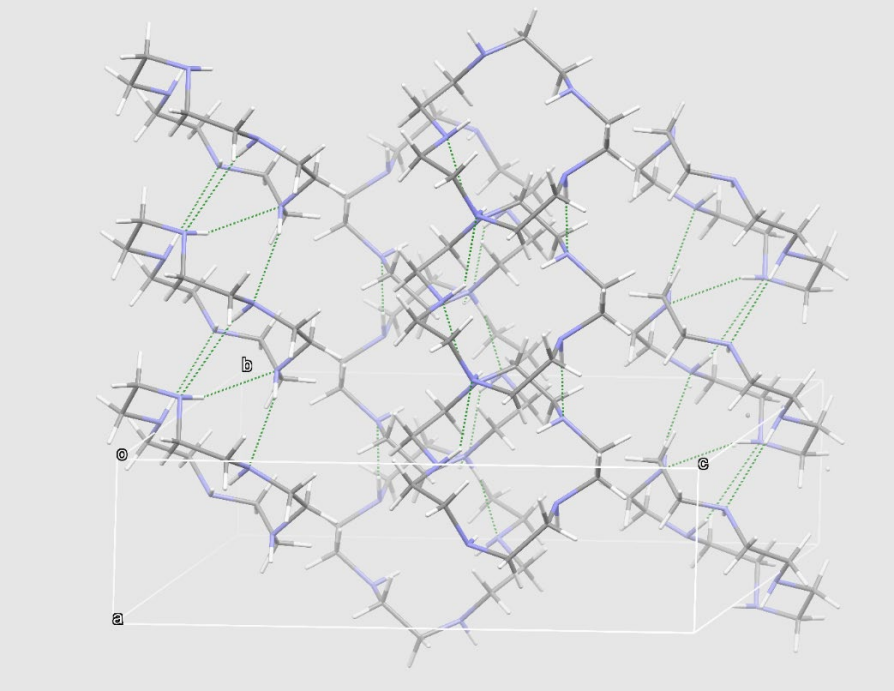

Figure L3b: Solid state packing of ADS102, **15aneN5**. Dashed lines show classical hydrogen bonds.

DGJ07B2 protonated ligand (15aneN5H$_3$)Cl$_2$(PF$_6$)

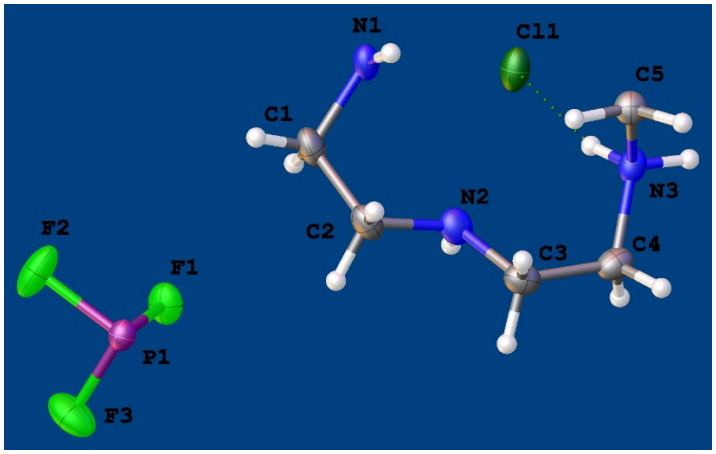

Figure L4: Asymmetric unit of DGJ07B2, (**15aneN5**H$_3$)Cl$_2$(PF$_6$), with atoms drawn as 50 % probability ellipsoids.

It is possible to protonate the **15aneN5** ligand and crystallise it as the hydrochloride/ hexafluorophosphate salt. This crystallises in the centric space group C2/c with one half of the **15aneN5**H$_3^{3+}$ ion in the asymmetric unit. The full molecule is generated by the *c*-glide as shown below in Figure L4b.

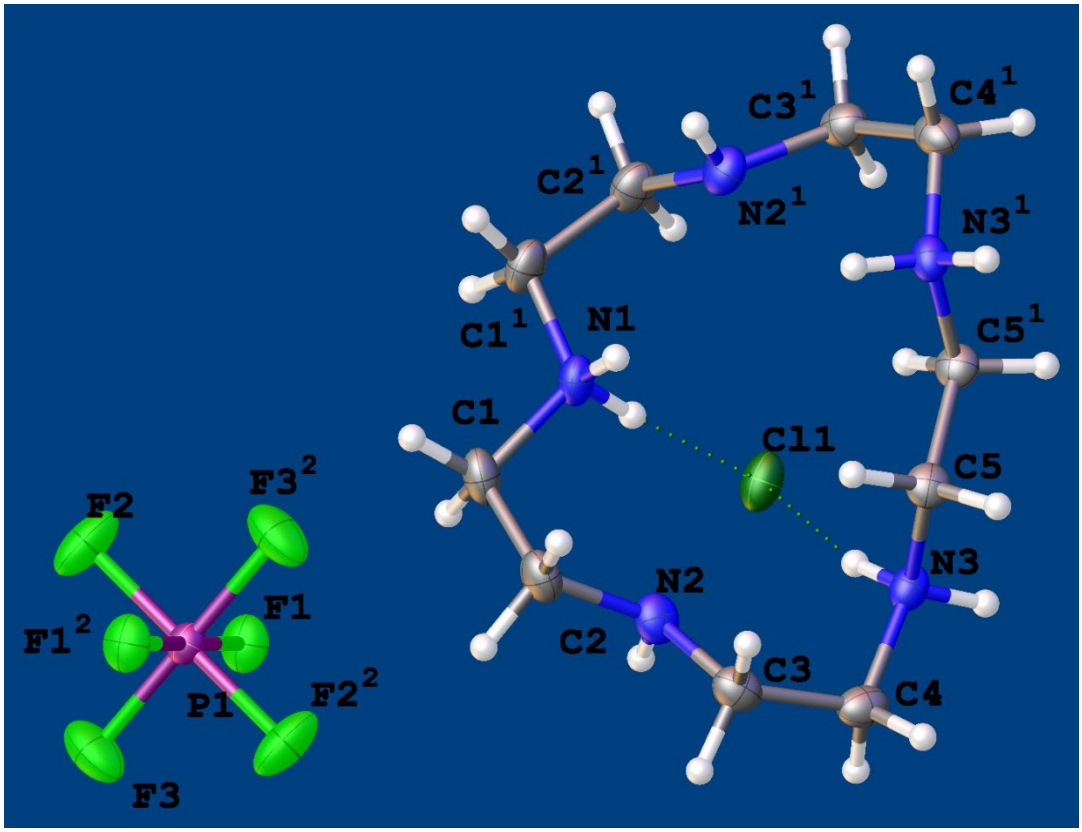

Figure L4b: Molecular structure of DGJ07B2, (**15aneN5**H_3)Cl_2(PF_6), with atoms drawn as 50 % probability ellipsoids. Symmetry operations used to generate equivalent atoms: 1 = –*x*, *y*, 3/2–*z*; 2 1/2–*x*, 1/2–*y*, 1–*z*.

In the solid state the protonated macrocycles pack in zigzag tapes that run parallel to the *c*-axis, with chloride between each cation. This generates a zigzag hydrogen-bonded tape that is sustained by $R^4_4(8)$ embraces that are augmented by further N-H…Cl hydrogen bonds. These tapes and the solid packing are shown below in Figure L4c and L4d. Between the tapes lie PF_6^- and there are C-H···F interactions between these and the macrocycles.

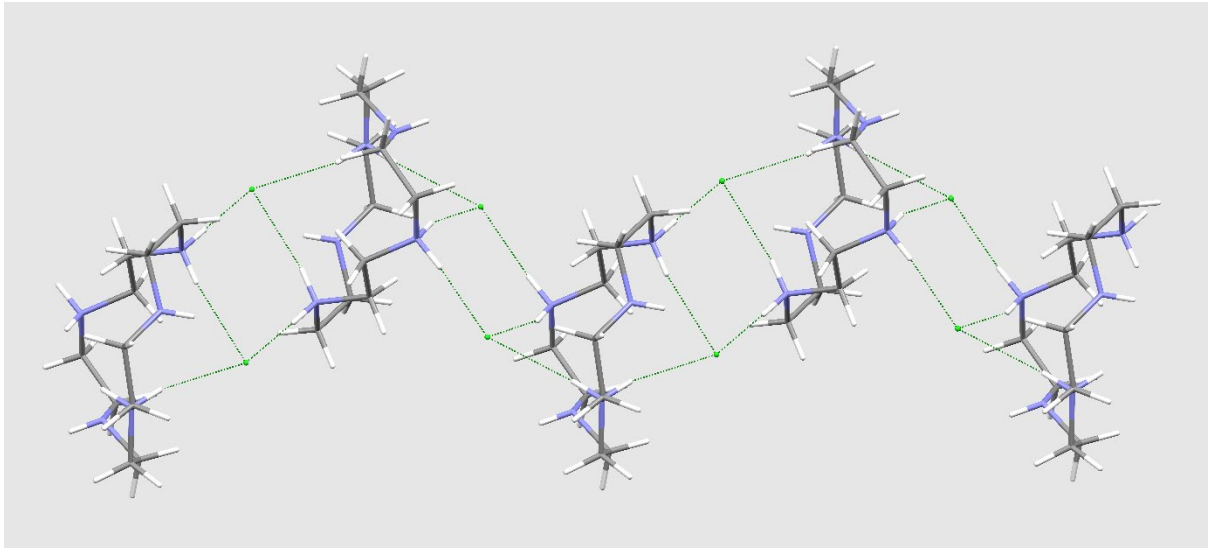

Figure L4c: Hydrogen-bonded tape present in DGJ07B2, (**15aneN5**H_3)Cl_2(PF_6). Dashed lines show N-H···Cl hydrogen bonds.

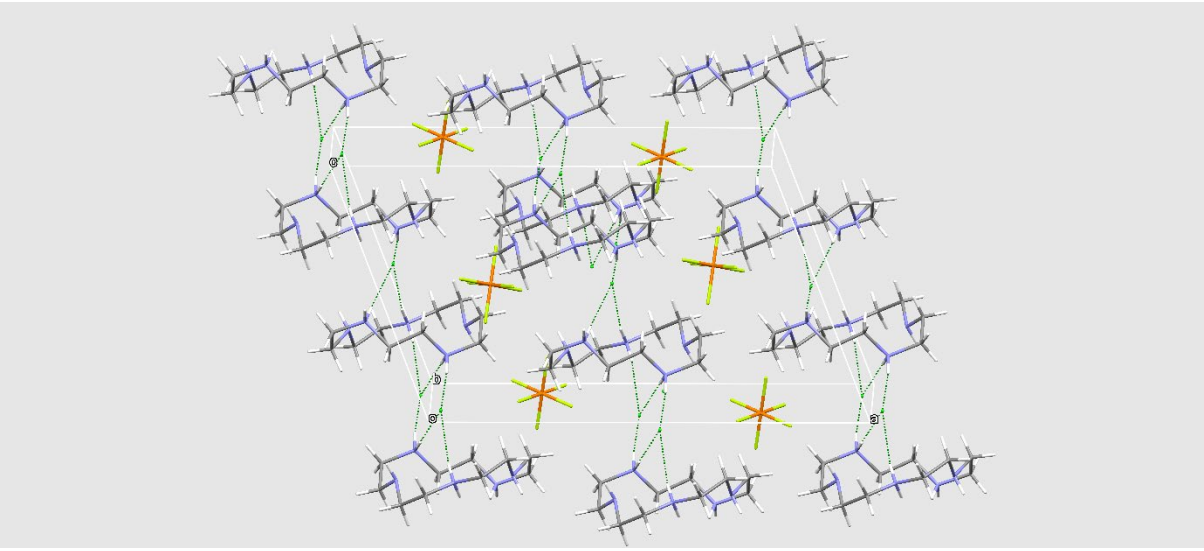

Figure L4d: Solid state packing in in DGJ07B2, (**15aneN5**H_3)Cl_2(PF_6). Dashed lines show N-H···Cl hydrogen bonds. For clarity the extensive C-H···F interactions present are not illustrated.

SECTION 2: CRYSTALLOGRAPHIC INFORMATION FOR METAL – 15aneN5 COMPLEXES

DGJ07B, [Cr(15aneN5)Cl]Cl(PF_6)

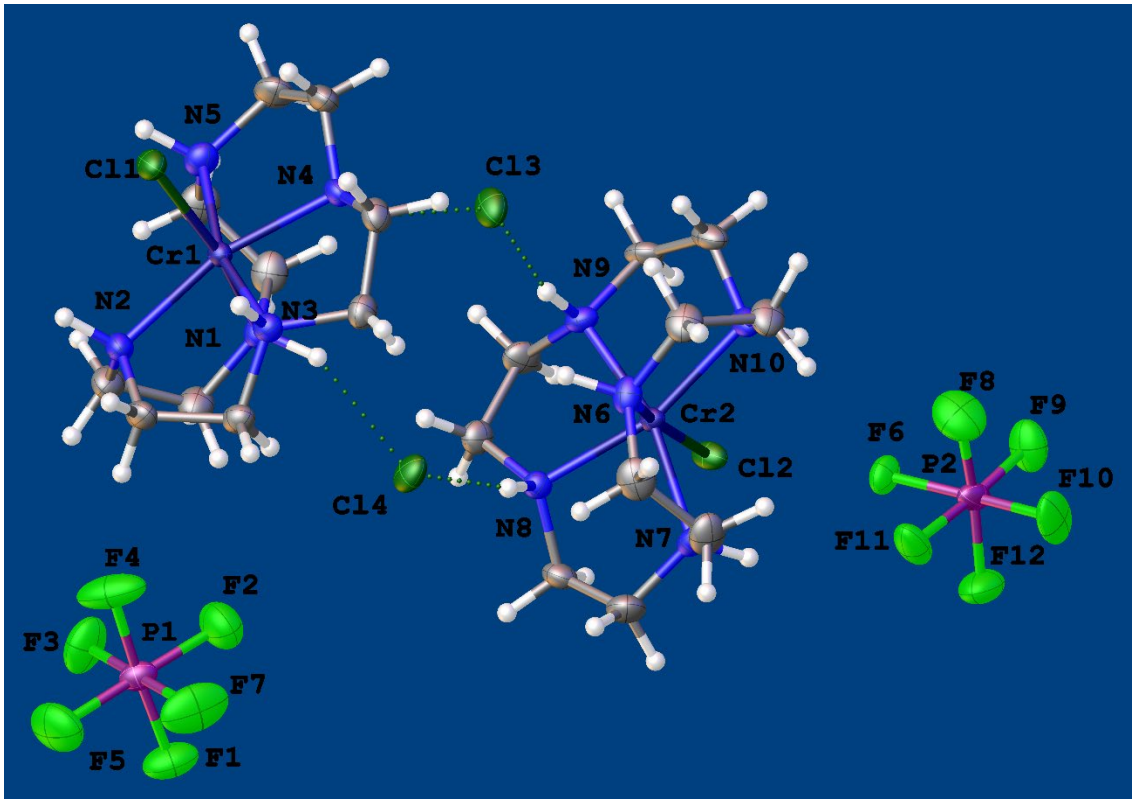

Figure S1: Asymmetric unit of DGJ07B, [Cr(**15aneN5**)Cl]Cl(PF_6), with atoms drawn as 50 % probability ellipsoids. Minor disorder is not shown.

A routine refinement in the centric space group P-1 was carried out. Minor disorder was treated using standard methods.

SWOSU069 (DR08), [Cr(**15aneN5**)Cl]$Cl_2(H_2O)$

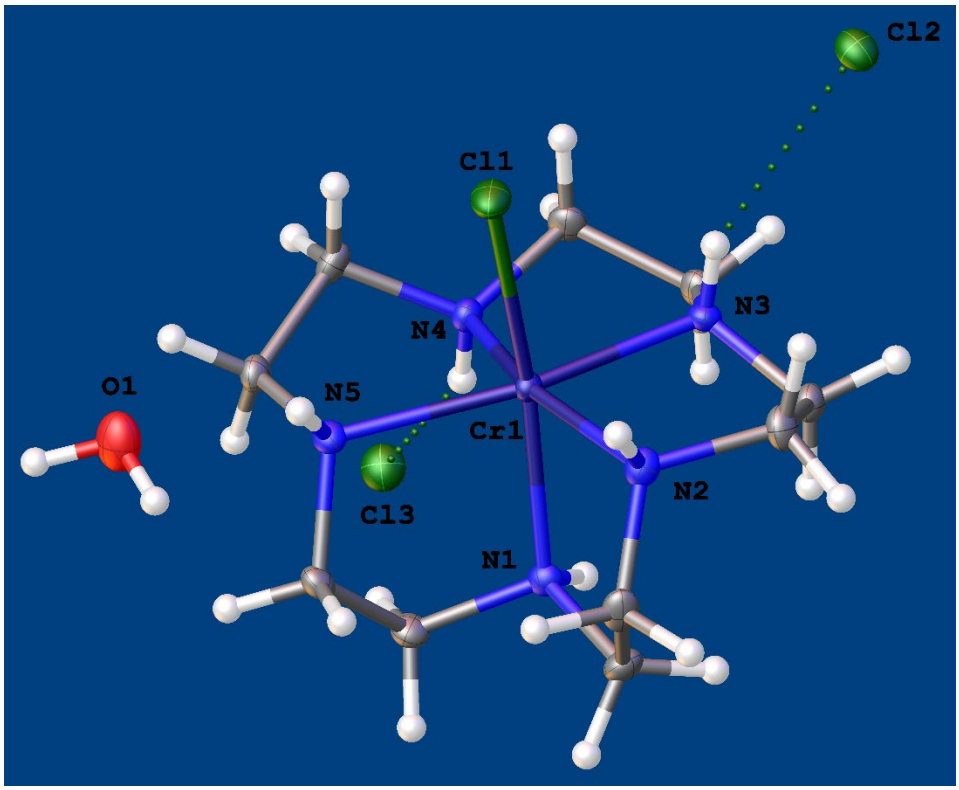

Figure S2: Asymmetric unit of SWOSU069 (DR08), [Cr(**15aneN5**)Cl]$Cl_2(H_2O)$ with atoms drawn as 50 % probability ellipsoids.

A routine refinement in the non-centric space group Cc was carried out. There is no evidence for a centre of symmetry. The Flack parameter was refined as 0.158(9).

MBA09, [Mn(**15aneN5**)NH_3]$(PF_6)_2$

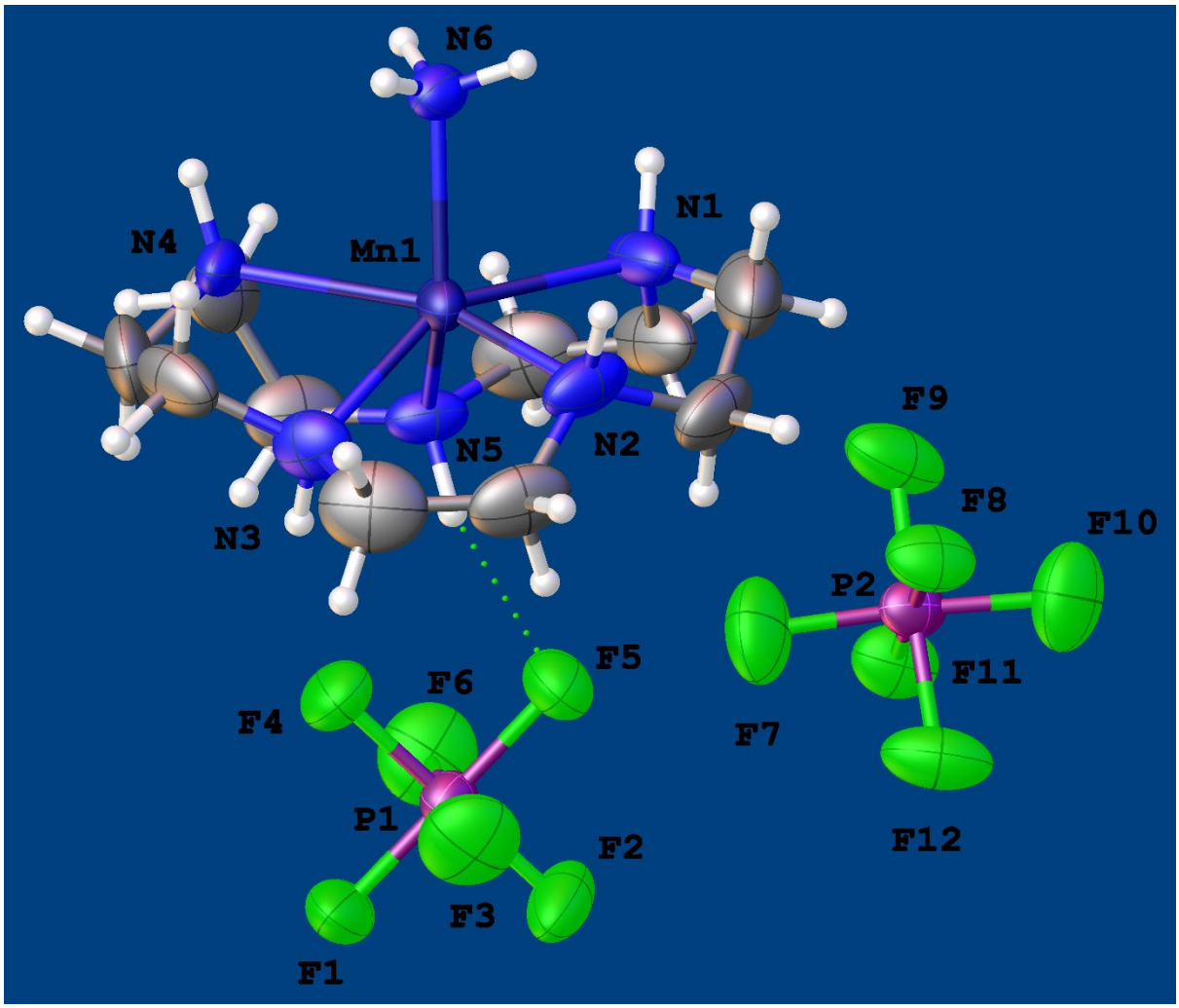

Figure S3: Asymmetric unit of MBA09, [Mn(**15aneN5**)NH_3]$(PF_6)_2$ with atoms drawn as 50 % probability ellipsoids. Disorder in the PF_6^- anions and the central complex is not shown.

[Mn(**15aneN5**)NH_3]$(PF_6)_2$ crystallises in the non-centric space group $P6_5$ and displays disorder both in the PF_6^- and in the orientation of the **15aneN5** ligand. There are two distinct orientations of the ligand, approximately related by a pseudo-mirror plane that runs through C1, Mn1, and C6. The two orientations were each present in 50 % occupancy. A representation of this disorder is shown below in Figure S3b. The high symmetry space group and presence of substantial disorder means the data-to-parameter ratio is somewhat lower than optimal. The bound ammonia was clearly identified from difference Fourier maps that indicated this was not bound water.

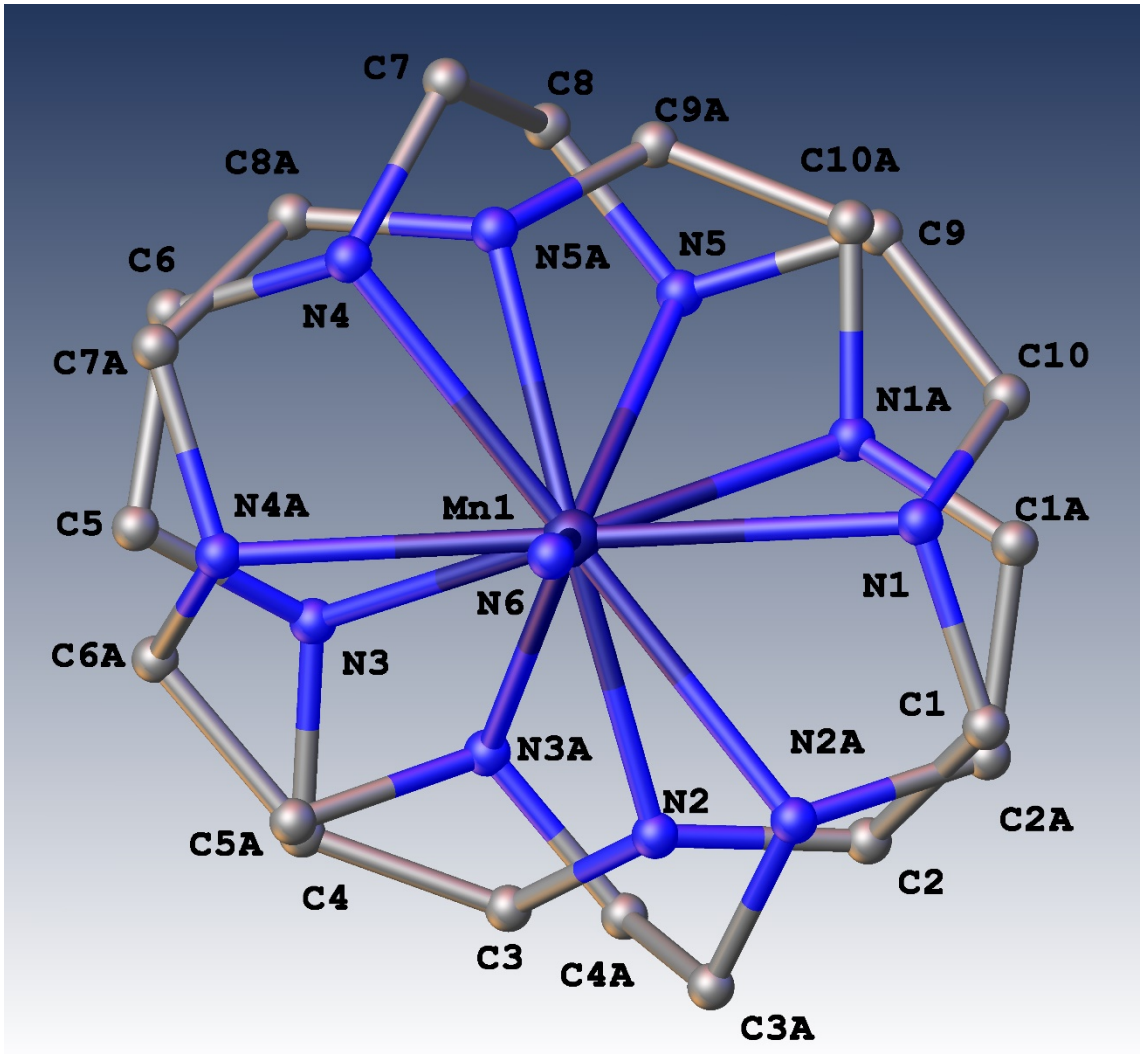

Figure S3b: Two orientations (each 50 % occupied) on the **15ne5N** ligand in [Mn(**15aneN5**)NH_3](PF_6).

Further details for MBA09, [Mn(**15aneN5**)NH_3](PF_6)

It is possible to carry out comparison refinements with water bound (H_2O) and with ammonia (NH_3) bound. Details of the fit in each case are shown below.

If water is present there is an excess of electron density on this site suggesting nitrogen rather than oxygen. (As shown in electron density maps in Olex2)
Furthermore, the ammonia forms three hydrogen bonds to PF_6^- anions in the structure, perhaps suggesting an energetic reason why this is observed. A figure helping to show this is below.

Details of refinement follow:

WATER

Data/restraints/parameters	5358/1299/384
Goodness-of-fit on F^2	1.026
Final R indexes [I>=2σ (I)]	R_1 = 0.0495, wR_2 = 0.1243
Final R indexes [all data]	R_1 = 0.0620, wR_2 = 0.1333
Largest diff. peak/hole / e $Å^{-3}$	0.55/-0.35
Flack parameter	0.04(4)

AMMONIA

Data/restraints/parameters	5358/1299/384
Goodness-of-fit on F^2	1.024
Final R indexes [I>=2σ (I)]	R_1 = 0.0478, wR_2 = 0.1168
Final R indexes [all data]	R_1 = 0.0601, wR_2 = 0.1251
Largest diff. peak/hole / e $Å^{-3}$	0.53/-0.34
Flack parameter	0.04(3)

A competitive refinement involving both water and ammonia is unstable.

We have chosen to retain the model with ammonia because it gives a very significantly better fit to wR_2 for both the strong data and for all data. eg wR_2 (all data) values are 0.1333 (H_2O) and 0.1251 (NH_3).

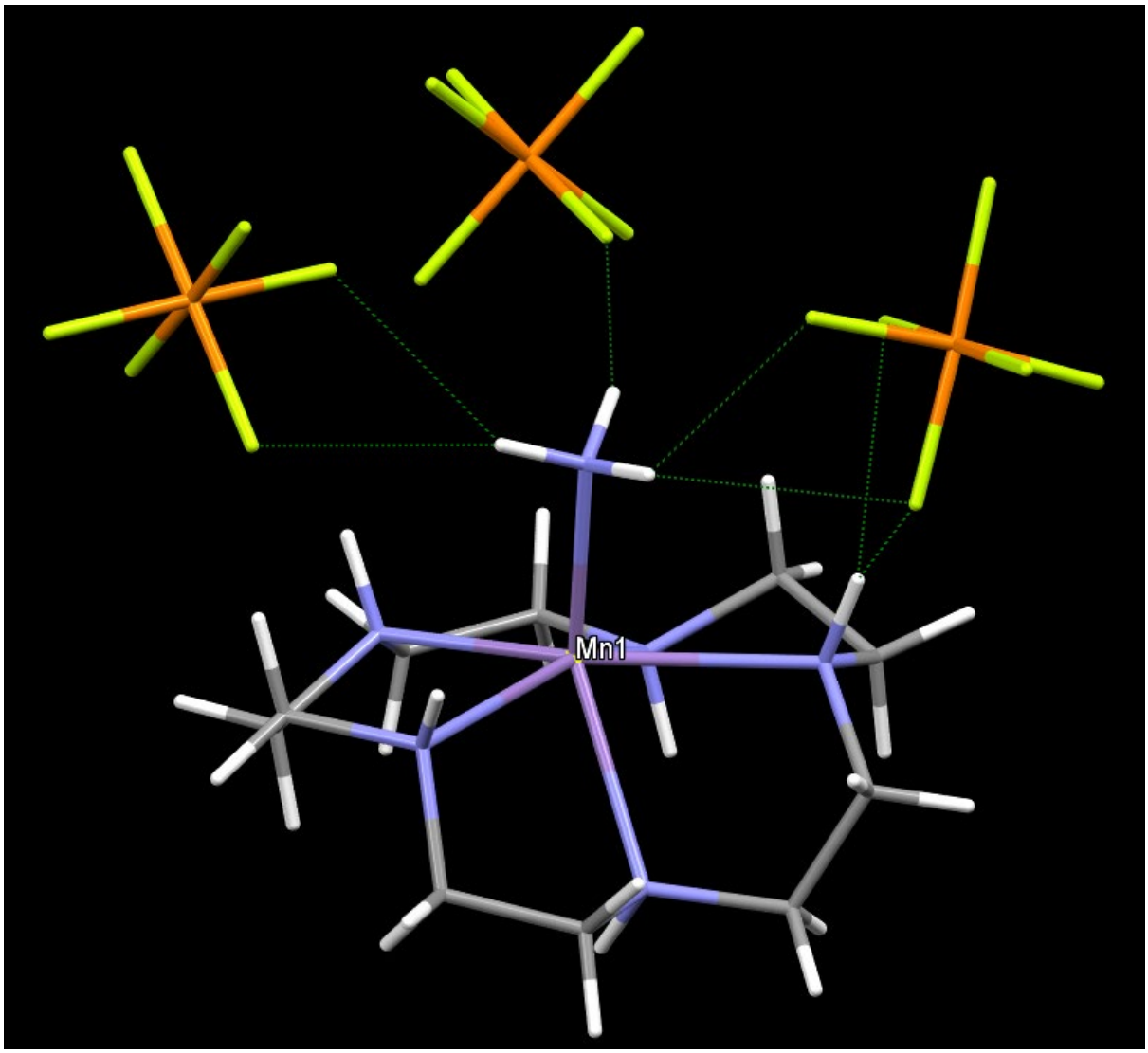

Figure S3c: Representation of MBA09, [Mn(**15aneN5**)NH_3](PF_6) showing the three sets of hydrogen bonds formed by bound ammonia to PF_6^-.

DD07a, [Fe(**15aneN5**)$(CH_3COO)_2$](PF_6)

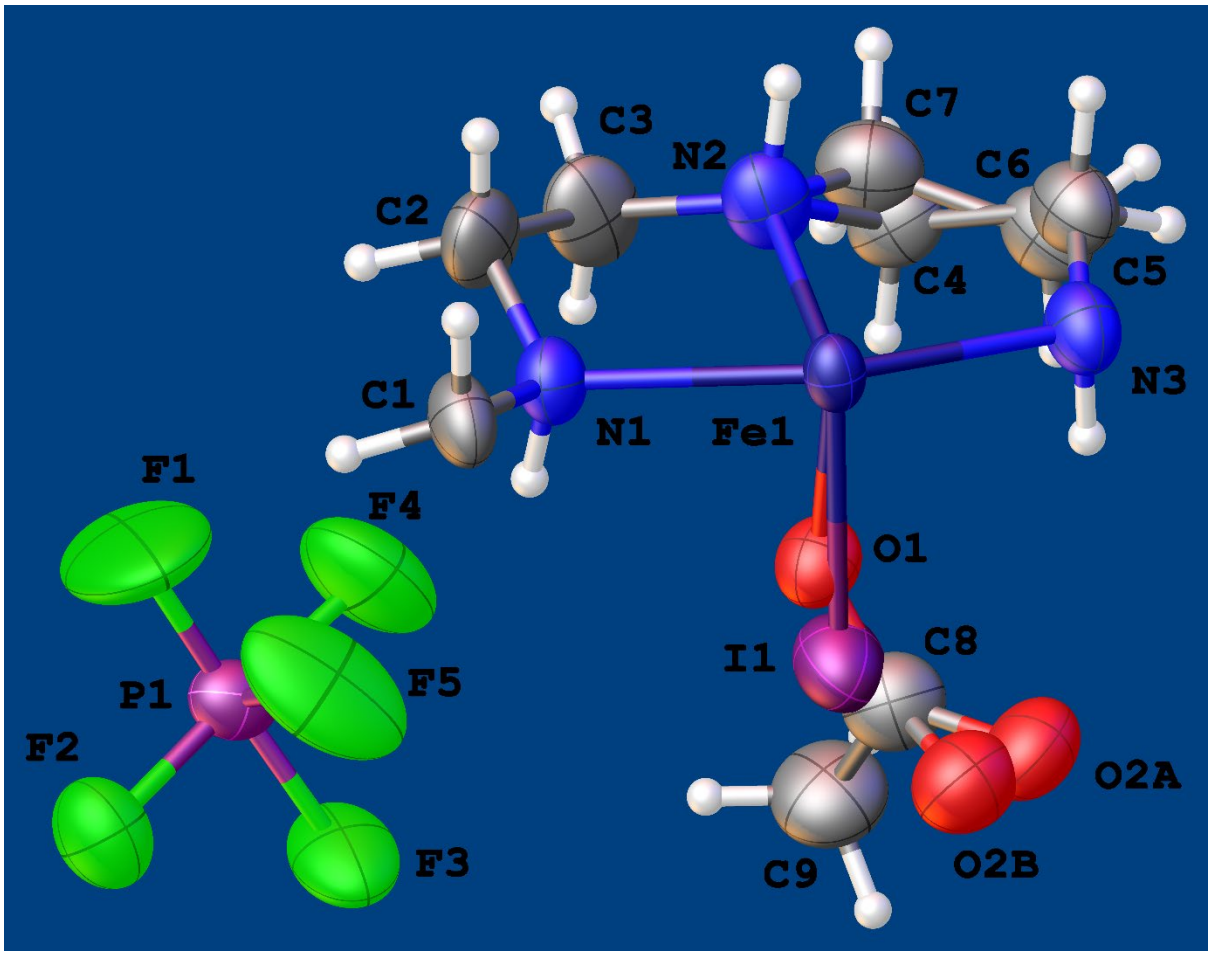

Figure S4: Asymmetric unit of DD07a, [Fe(**15aneN5**)$(CH_3COO)_2$](PF_6), with atoms drawn as 50 % probability ellipsoids. Disorder in the PF_6^- anions and the central complex is not shown.

The structure determination of the iron complex DD07a, [Fe(**15aneN5**)$(CH_3COO)_2$](PF_6), is crystallographically complicated because the complex sits on a site that is higher symmetry than that of the ligand; this introduces disorder and two orientations of the ligand at the metal. There is further small-scale disorder in the anion and there is evidence for around 6 % of iodide replacing acetate bound at the metal.

The whole complex generated by the symmetry operations of the space group is shown in figure 4b.

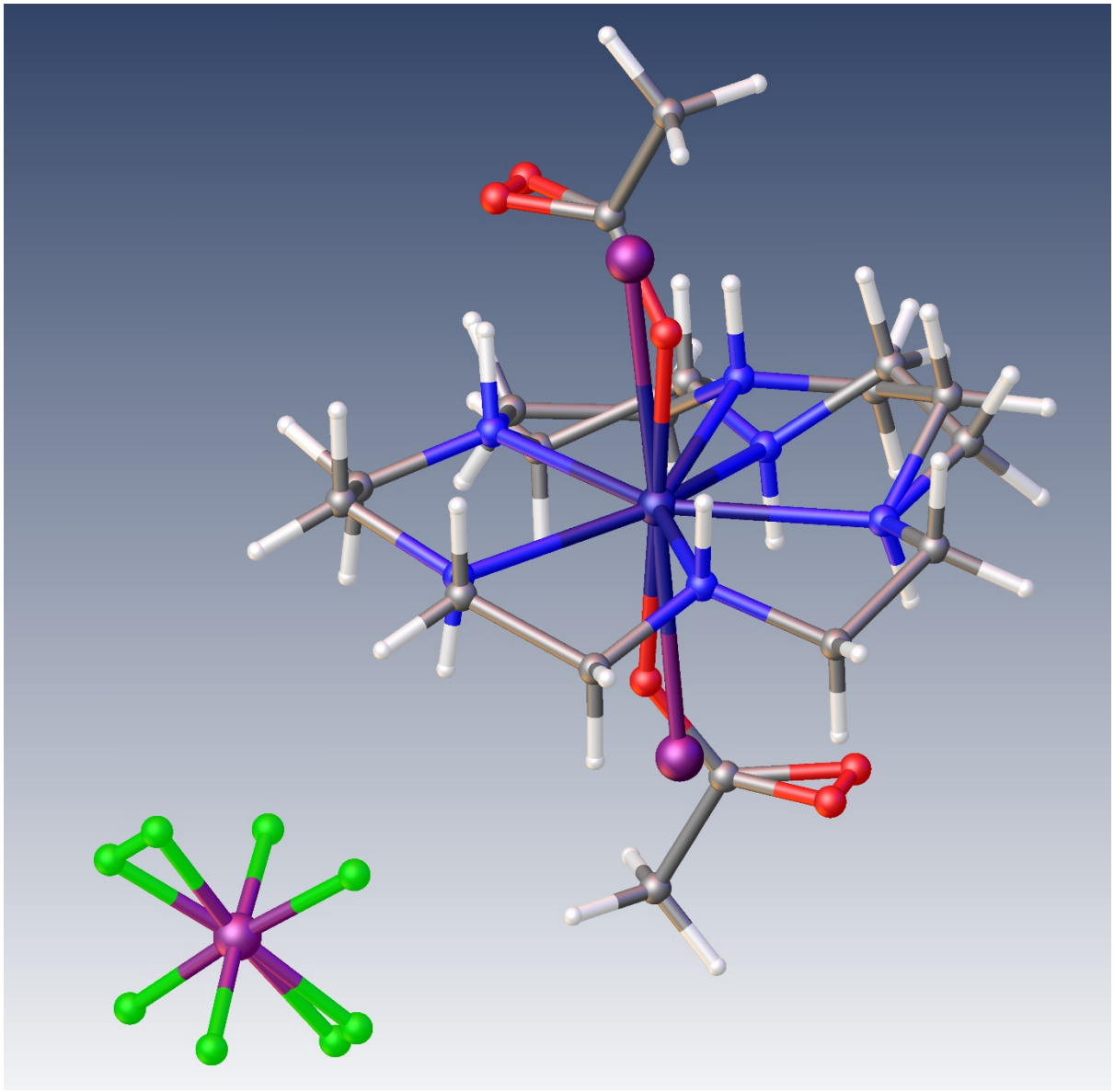

Figure S4b: Expanded asymmetric unit of DD07a, [Fe(**15aneN5**)$(CH_3COO)_2$](PF_6). All of the different disorder components are shown. (Colours as for Fig S4)

ALB04, [Fe(**15aneN5**)Cl_2]

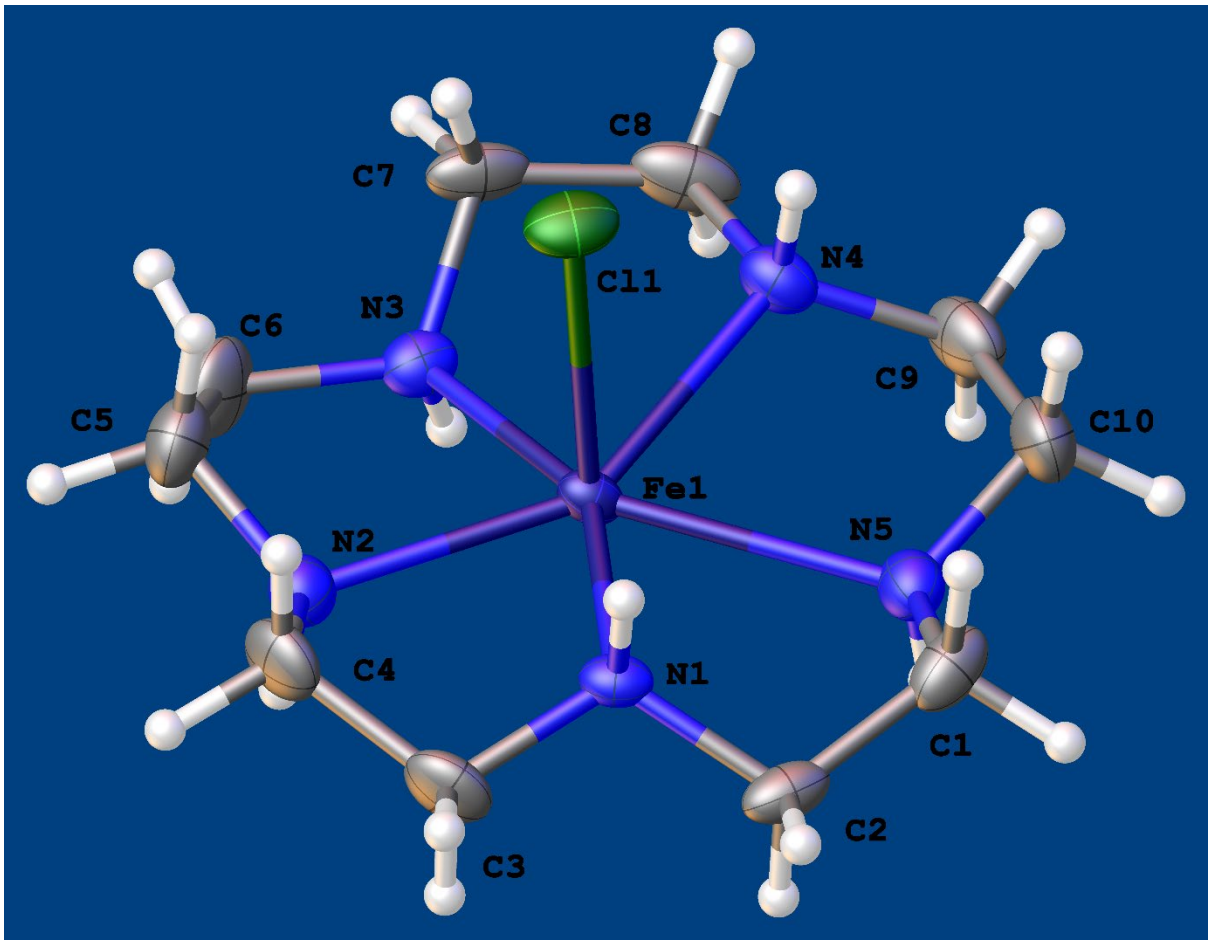

Figure S5: Asymmetric unit of ALB04, [Fe(**15aneN5**)Cl_2] with atoms drawn as 50 % probability ellipsoids.

The complex crystallises in the centric space group $P2_1/n$. The central Fe^{2+} is located on a centre of inversion; this generates the second bound chloride ion, but also generates a second orientation of the ligand. Therefore, in the solid each Fe^{2+} is 7-coordinate but there are two orientations of the ligand and these occur at random in equal amounts.

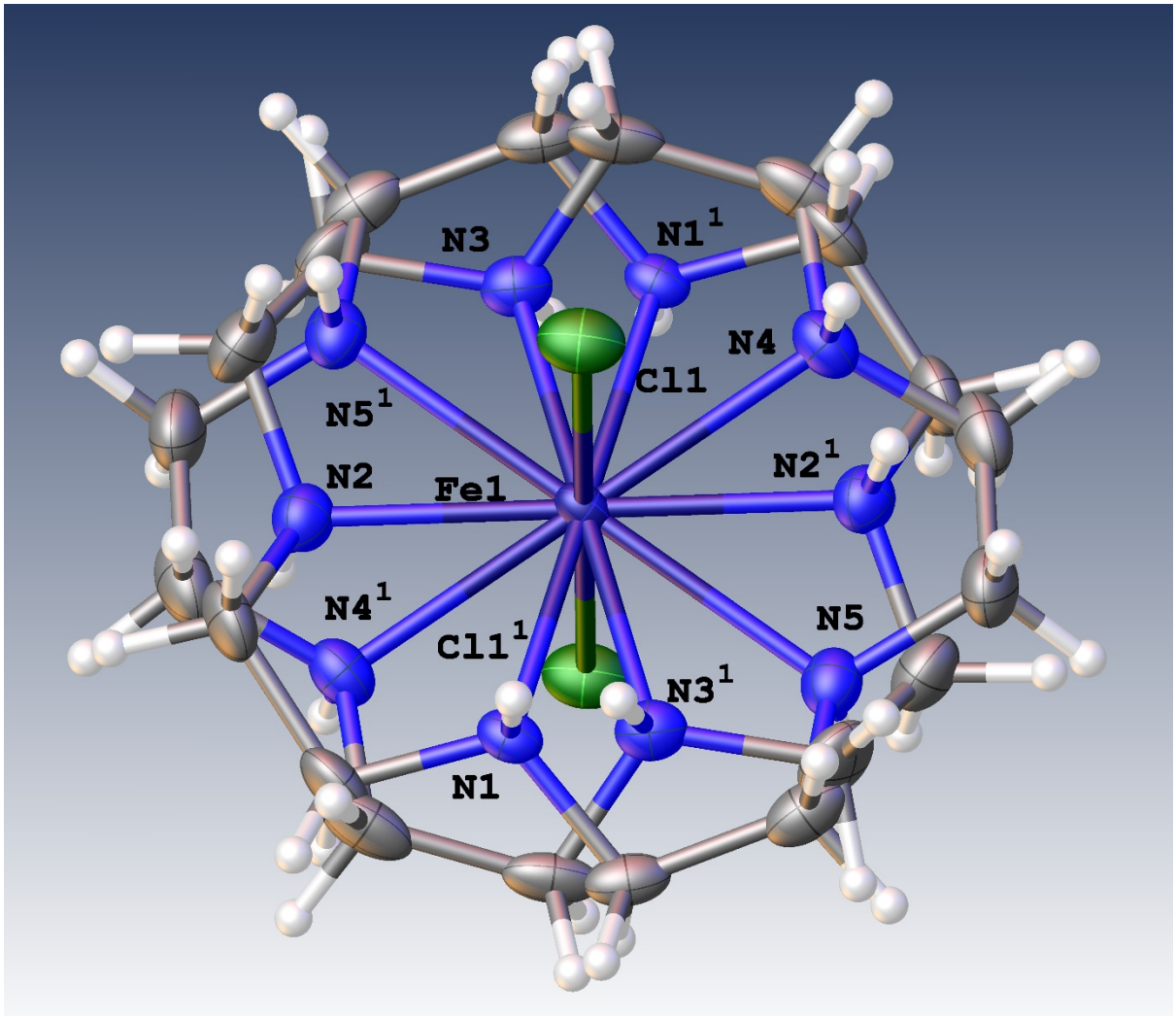

Figure S5b: [Fe(**15aneN5**)Cl_2] with two orientations of ligand shown. Symmetry operation to generate equivalent atoms: 1 = 1–x, –y,–z.

DSB04A, [Co(**15aneN5**)]-µCl-[$CoCl_3$]

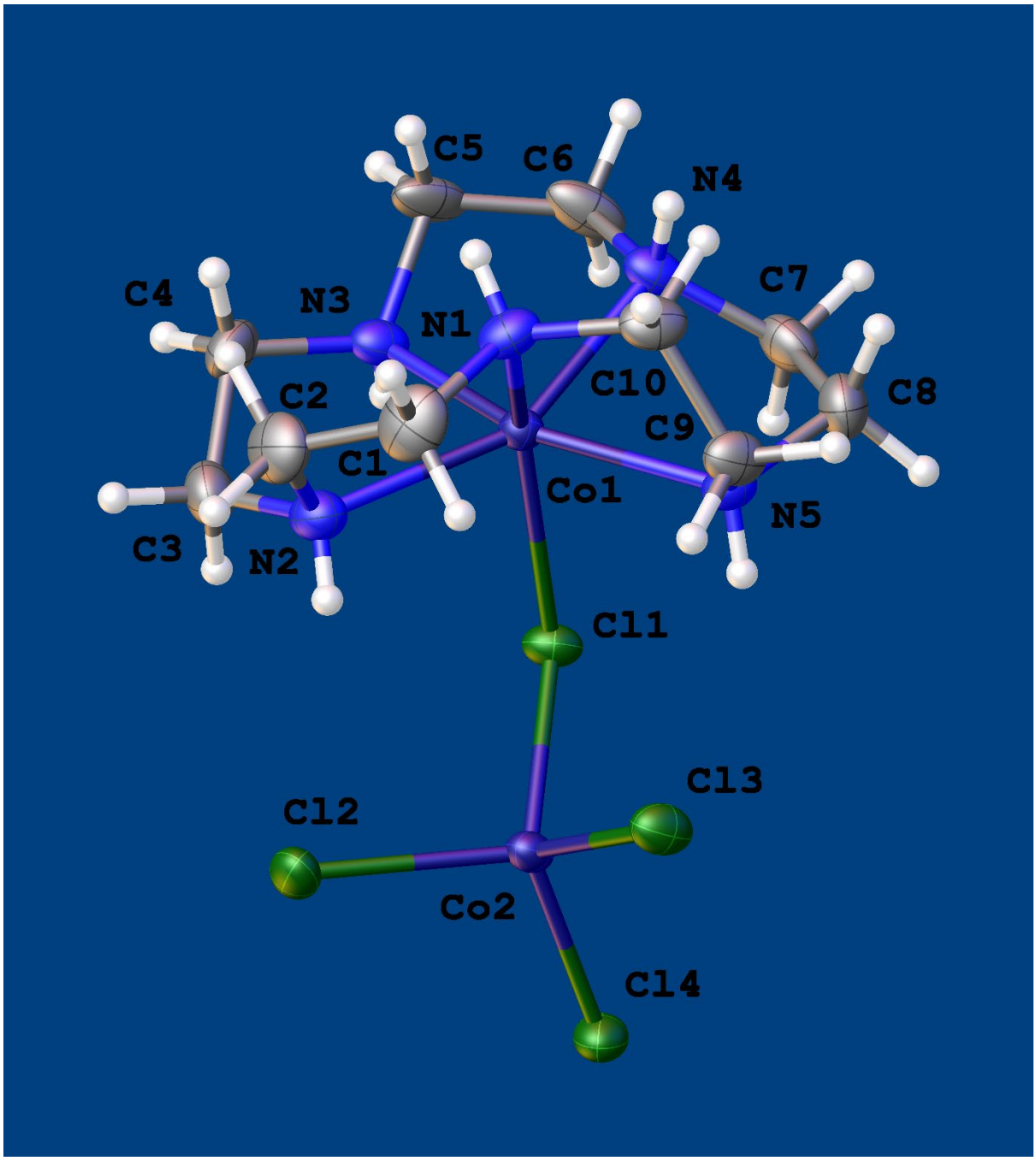

Figure S6: Asymmetric unit of DSB04A, [Co(**15aneN5**)]-µCl-[$CoCl_3$] with atoms drawn as 50 % probability ellipsoids.

The structure is non-centric and crystallises in $P2_12_12_1$. The Flack parameter effectively refined to zero within error: 0.014(12).

DSB04B, [Co(**15aneN5**)Cl]$_2$[CoCl$_4$]

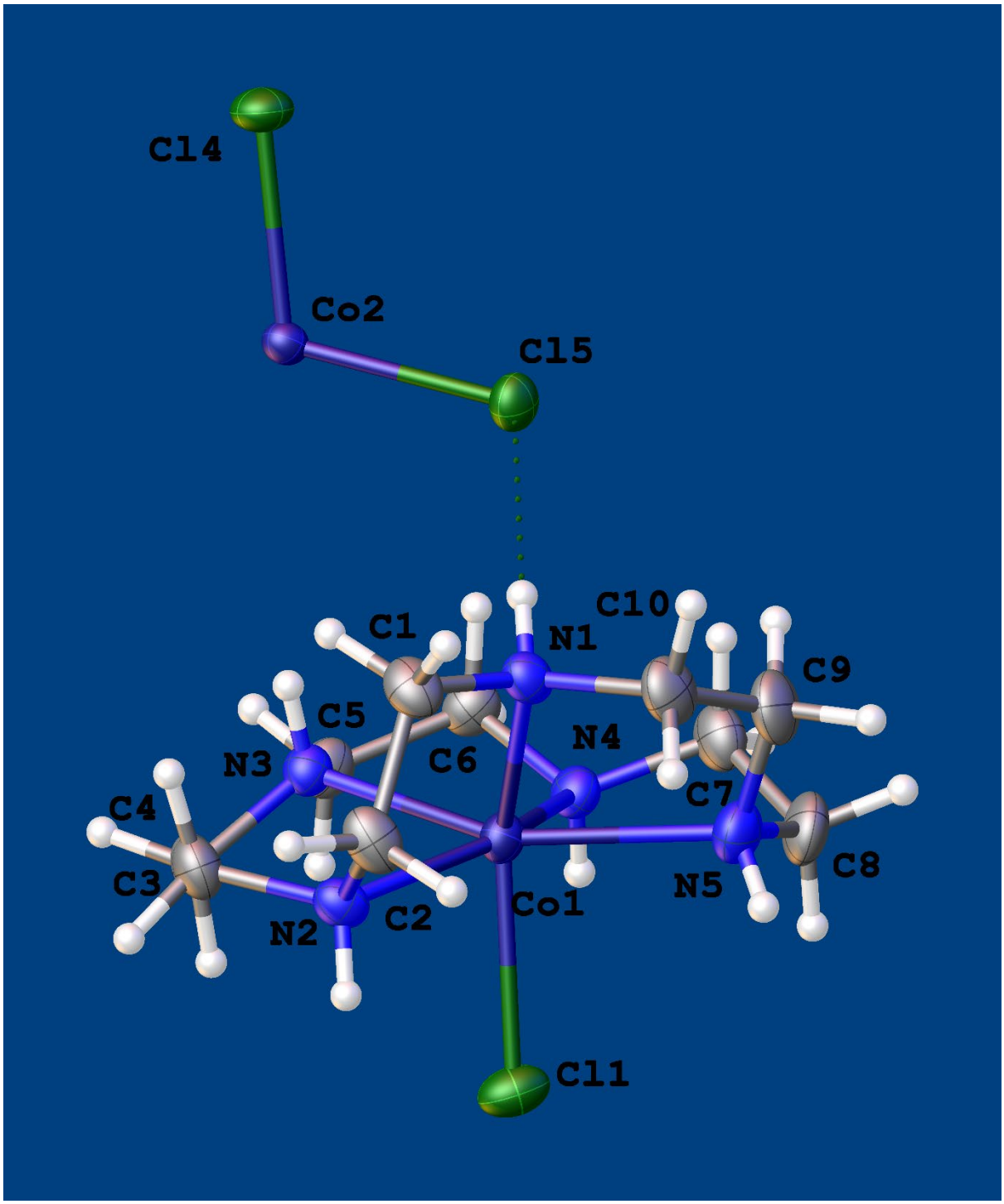

Figure S7: Asymmetric unit of DSB04B, [Co(**15aneN5**)Cl]$_2$[CoCl$_4$] with atoms drawn as 50 % probability ellipsoids.

A routine refinement in C2/c was performed. A single badly-fitted reflection was omitted from the final cycles of refinement. The asymmetric unit contains a single [Co(**15aneN5**)Cl] complex and one half of the $[CoCl_4]^{2-}$ anion, the second half of which is generated by the 2-fold rotation axis.

DSB04C, [Co(**15aneN5**)Cl]Cl

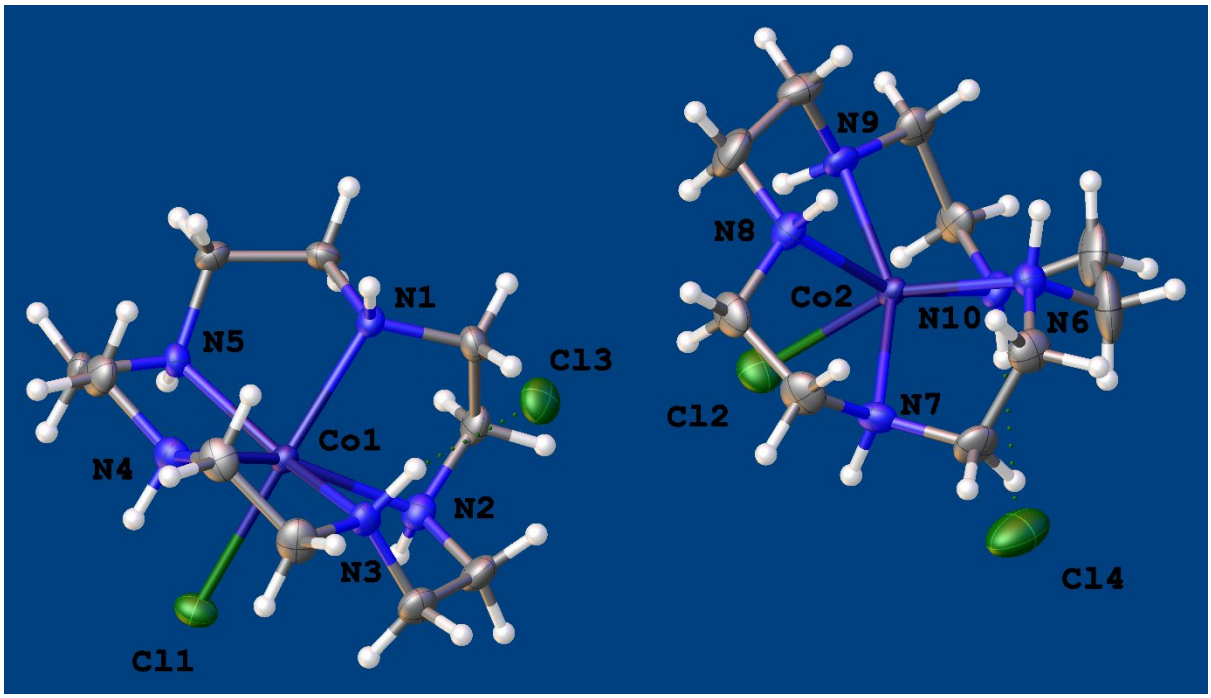

Figure S8: Asymmetric unit of DSB04C, [Co(**15aneN5**)Cl]Cl with atoms drawn as 50 % probability ellipsoids. Minor disorder is not represented.

A routine refinement in Pbca was performed. A single badly-fitted reflection was omitted from the final cycles of refinement. Small-scale disorder was treated using standard methods.

AF07, [Ni(**15aneN5**)(CH_3COO)](PF_6)

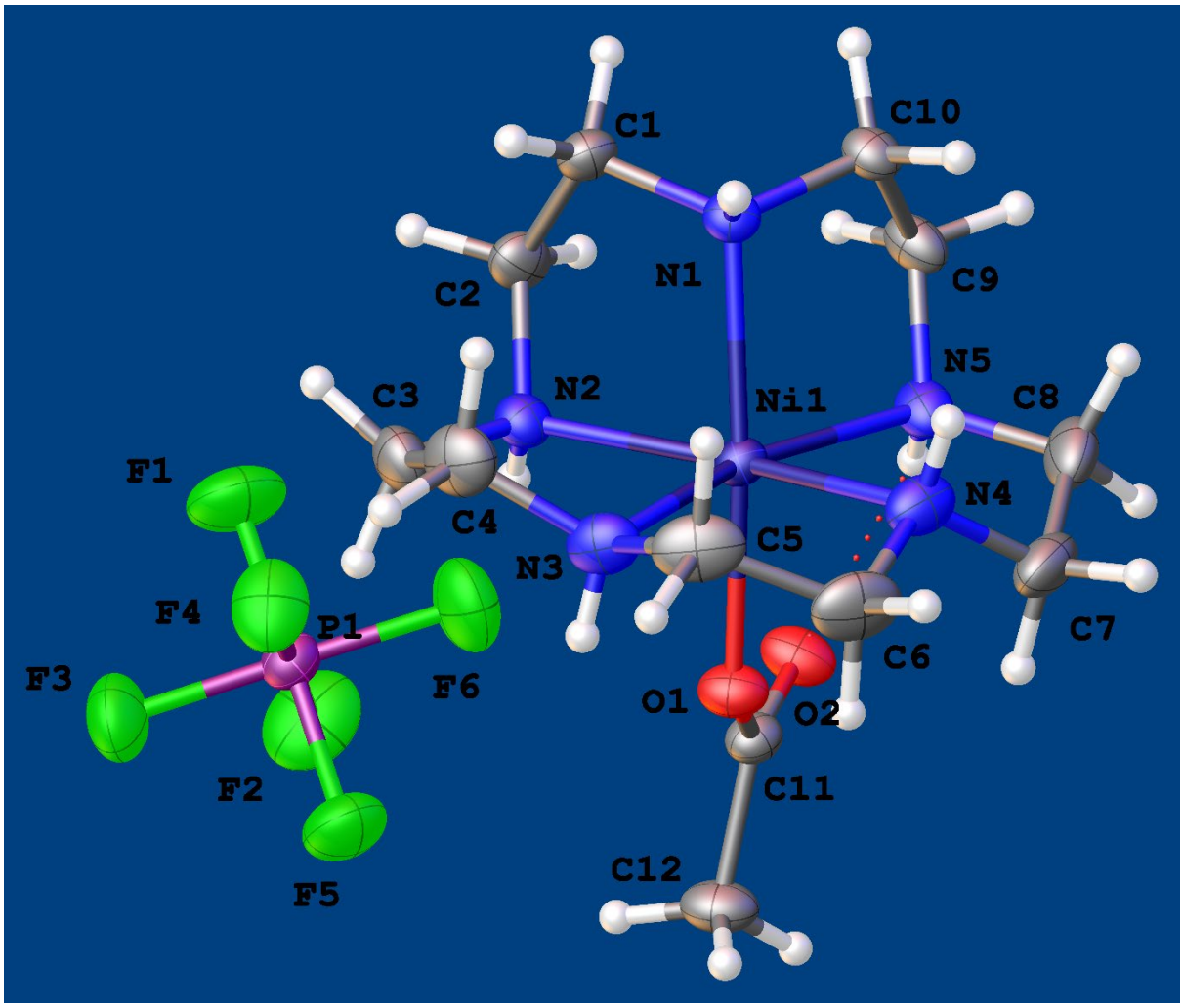

Figure S9: Asymmetric unit of AF07, [Ni(**15aneN5**)(CH_3COO)](PF_6) with atoms drawn as 50 % probability ellipsoids

This was refined in the space group $P2_12_12_1$ as a racemic twin with twin fraction 0.365(11).

KS11, [Cu(**15aneN5**)]$(PF_6)_2(CH_3NO_2)_2$

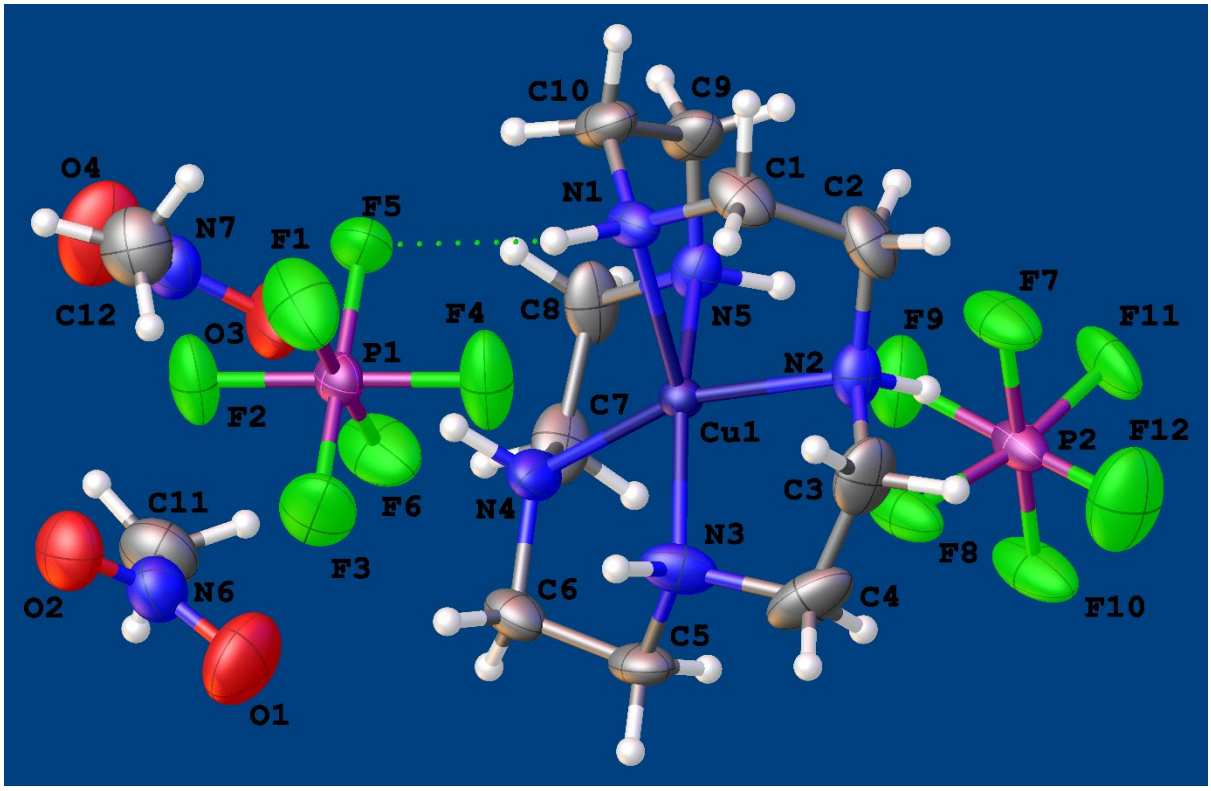

Figure S10: Asymmetric unit of KS11, [Cu(**15aneN5**)]$(PF_6)_2(CH_3NO_2)_2$ with atoms drawn as 50 % probability ellipsoids. Small-scale disorder in the anions is not shown.

This was refined in the space group $P2_1$as a racemic twin with twin fraction 0.44(9).

JE07, [Zn(**15aneN5**)]Cl_2

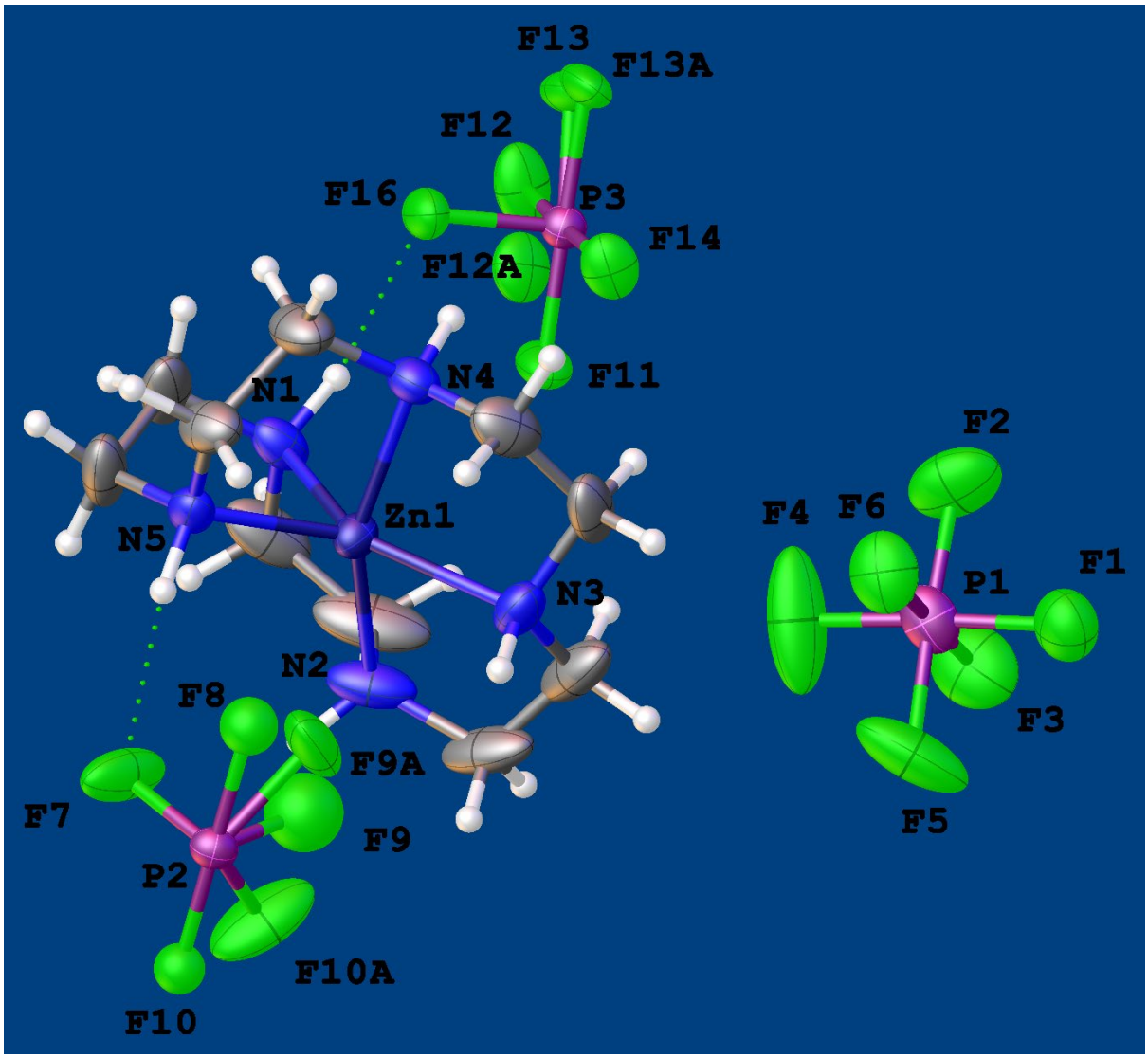

Figure S11: Asymmetric unit of JE07, [Zn(**15aneN5**)]Cl_2 with atoms drawn as 40 % probability ellipsoids. Small-scale disorder in the anions is represented; each independent atoms position in the disorder model is shown.

The structure was refined in the setting I2/a and the refinement was greatly complicated by the presence of disorder in the anions. The anion centred on P1 has one orientation, but the anions centred on P2 and P3 (each one half occupied) have multiple orientations. The anion containing P2 has two orientations (0.36:0.64) related by rotation of about 45 °about the P2-F7 bond. The anion containing P3 has three orientations (0.295, 0.295, 0.41) related by rotation of about 22.5 ° about the P13-F16 bond.

There was some evidence for twinning (twofold rotation about the 101 direction) and final refinements used a second twin component (twin fraction 0.0115(7)) and employed the HKLF5 formalism.

MG07B, [Ru(**15aneN5-diimine**)Cl](PF$_6$)

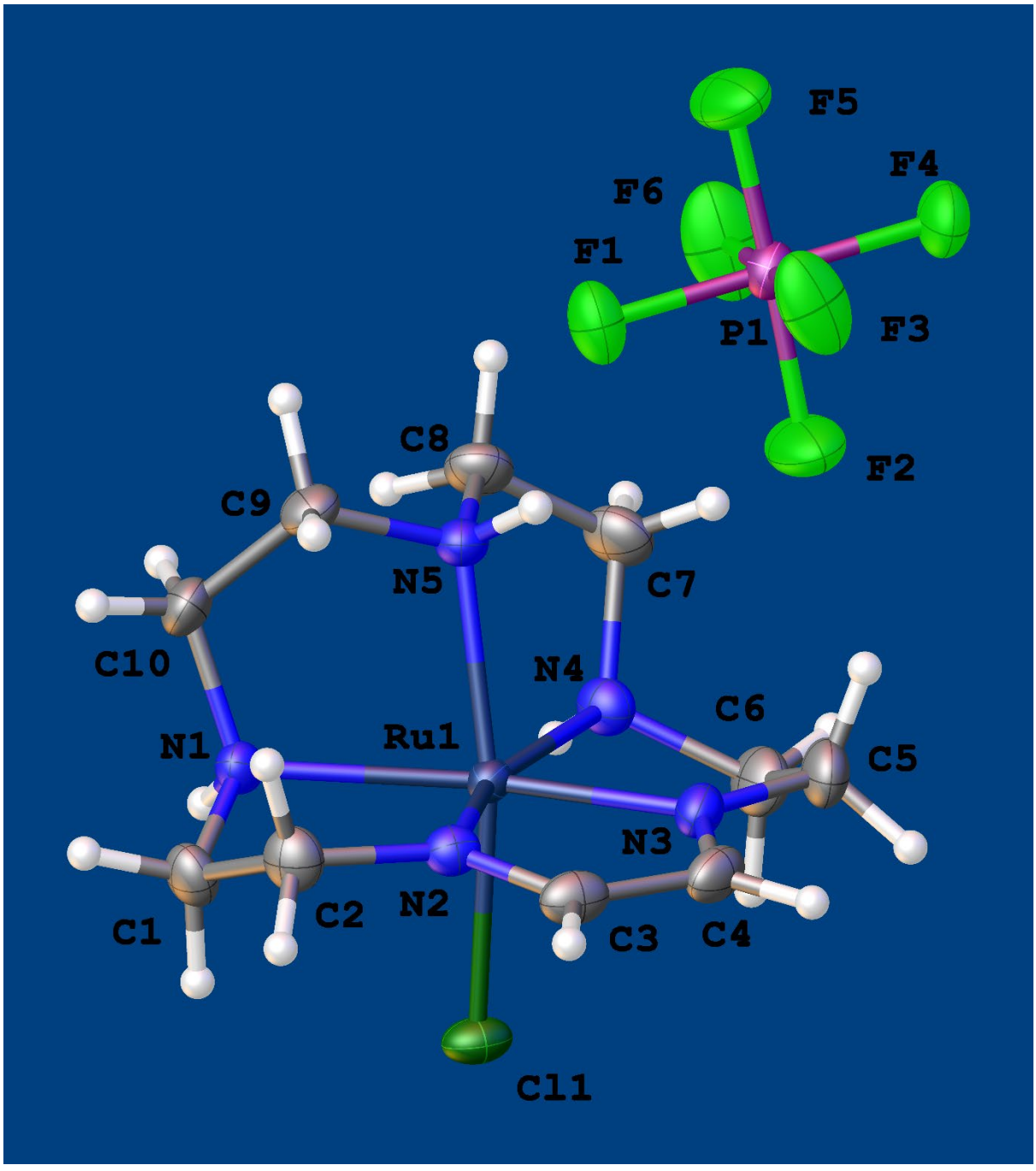

Figure S12: Asymmetric unit of KS11, MG07B, [Ru(**15aneN5-diimine**)Cl](PF$_6$) with atoms drawn as 50 % probability ellipsoids. Small-scale disorder in the anions is not shown.

C3=N2 and C4=N3 are the imine links present in the oxidised macrocycle.

Analysis of Cyclen, imCyclen, and 15ane5-diimine metrical parameters for bond lengths and angles at the macrocycle nitrogen atoms is a useful exercise.

The coordination of the cyclen in cis-V fashion at Ru^{2+} clearly introduces strain into the molecule. One way of visualising this is to plot the two C–N bond lengths against the C–N–C bond angle at each nitrogen. For an undistorted cyclen one would expect a C–N bond length around 1.5 Å and a bond angle close to 110 °. The distortion in the cyclen in WEMFUQ is easily visualised in the plot below; two nitrogens are rather distorted from the ideal geometry.

[Ru(15aneN5-diimine)Cl](PF_6) has a clear differentiation between the C–N and C=N geometry. The C–N=C is clearly visible with bond angle around 125 °.

The data for RIFTAB are not so clear; there are clearly secondary amines present, but two of the bonds are intermediate between amine and imine. We suspect this is because of disorder in the bonding that has not been modelled.

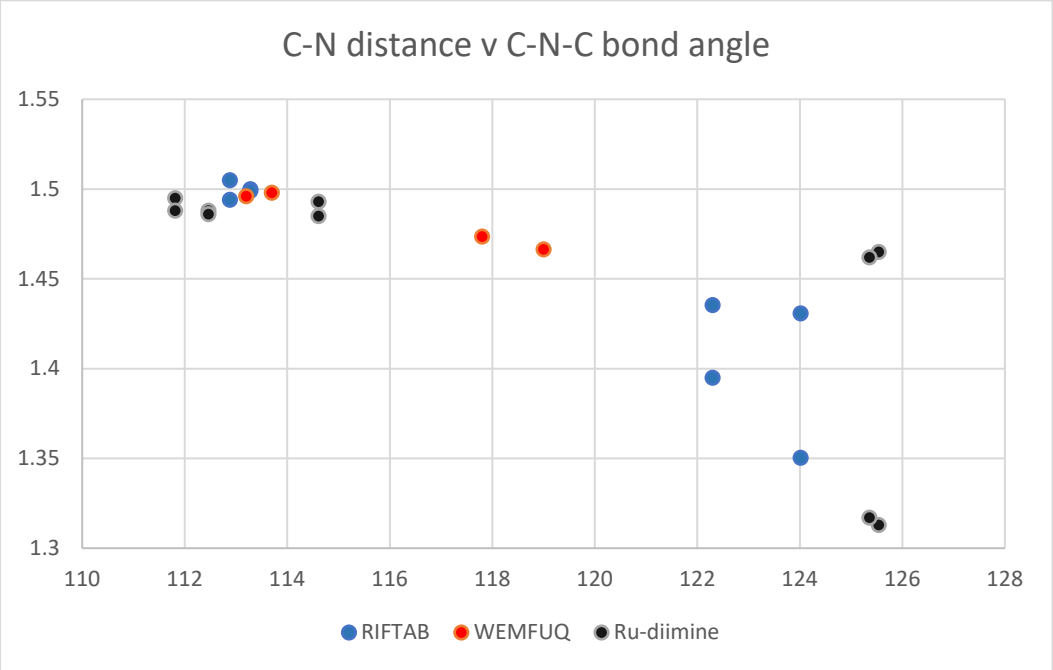

Figure S12b: Scatter plot to show bond length v bond angle at nitrogen for RIFTAB, WEMFUQ, and [Ru(15aneN5-diimine)Cl](PF_6).

WEMFUQ: [Ru(bipy)(cyclen)]Cl_2
Yuan-Jang Chen, Puhui Xie, M.J.Heeg, J.F.Endicott, Inorganic Chemistry, 2006, 45, 6282, DOI: 10.1021/ic0602547

RIFTAB: $[(tpt)_4(RuL)_6]^{12+}$
G.-H. Ning, Y. Inokuma and M. Fujita, *Chemistry - An Asian Journal*, 2013, **8**, 2596-2599.

SECTION 3: Characterization data for [Ru(15aneN5-diimine)Cl](PF$_6$)

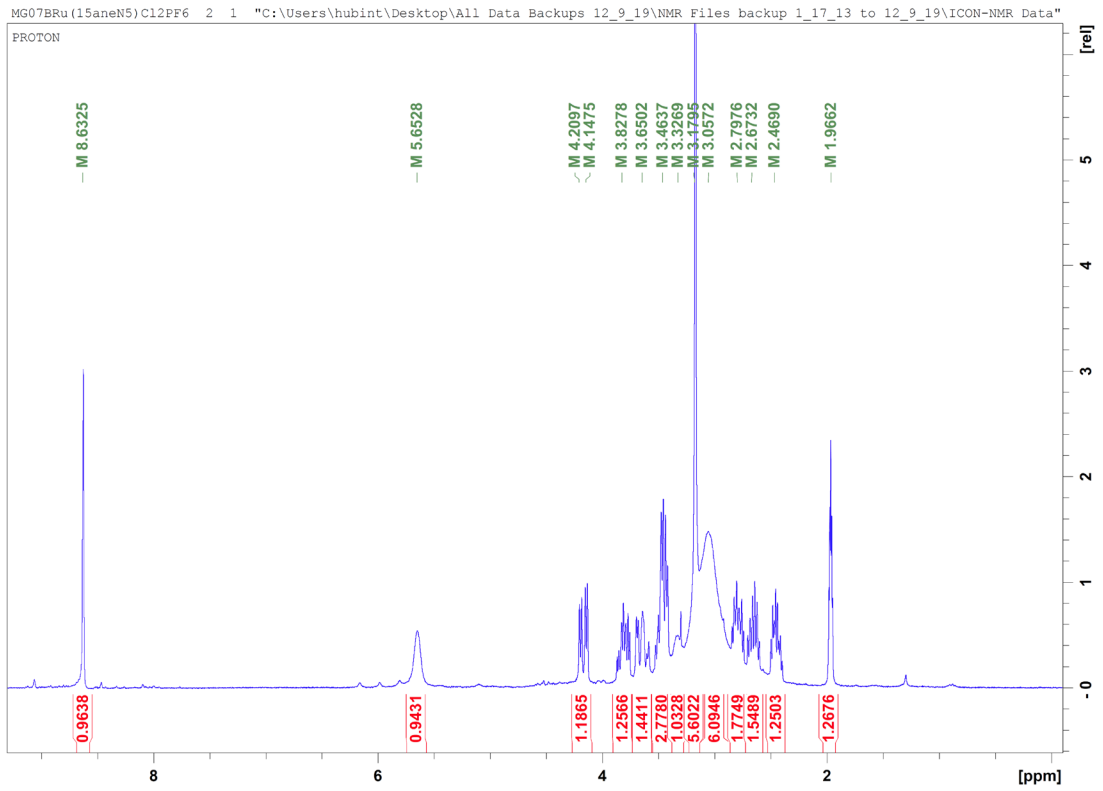

Figure S13: Proton NMR in CD_3CN of MG07B, [Ru(**15aneN5-diimine**)Cl](PF$_6$)

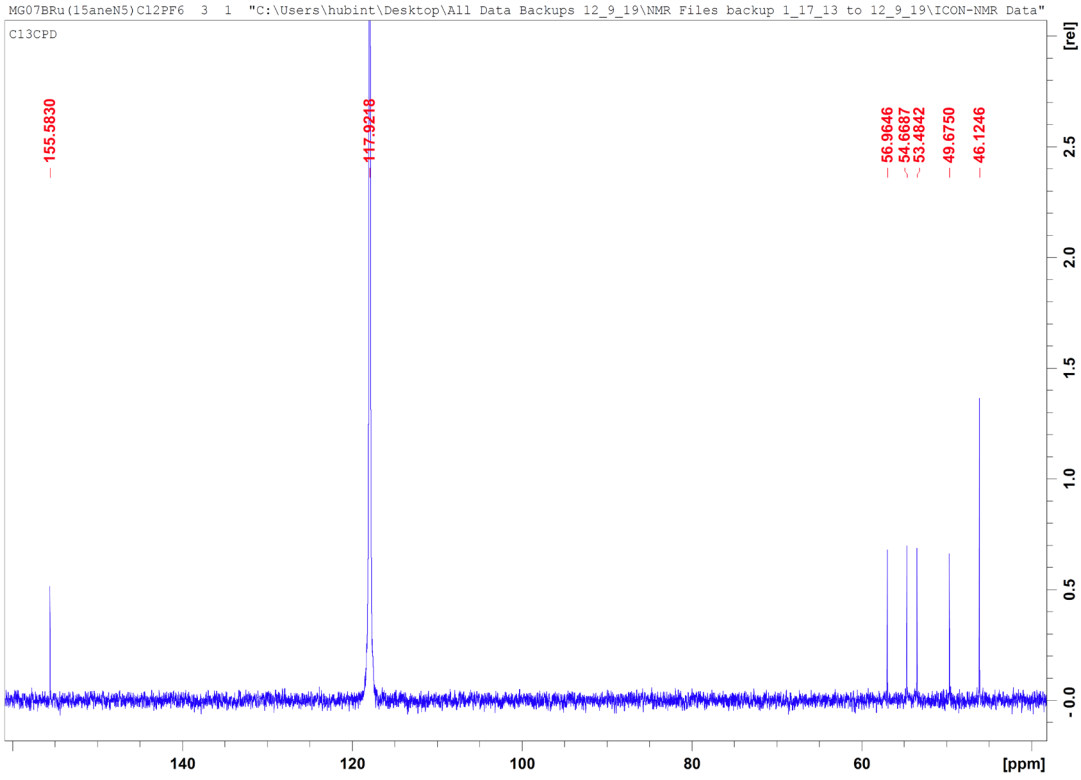

Figure S14: ^{13}C NMR in CD_3CN of MG07B, [Ru(**15aneN5-diimine**)Cl](PF$_6$)

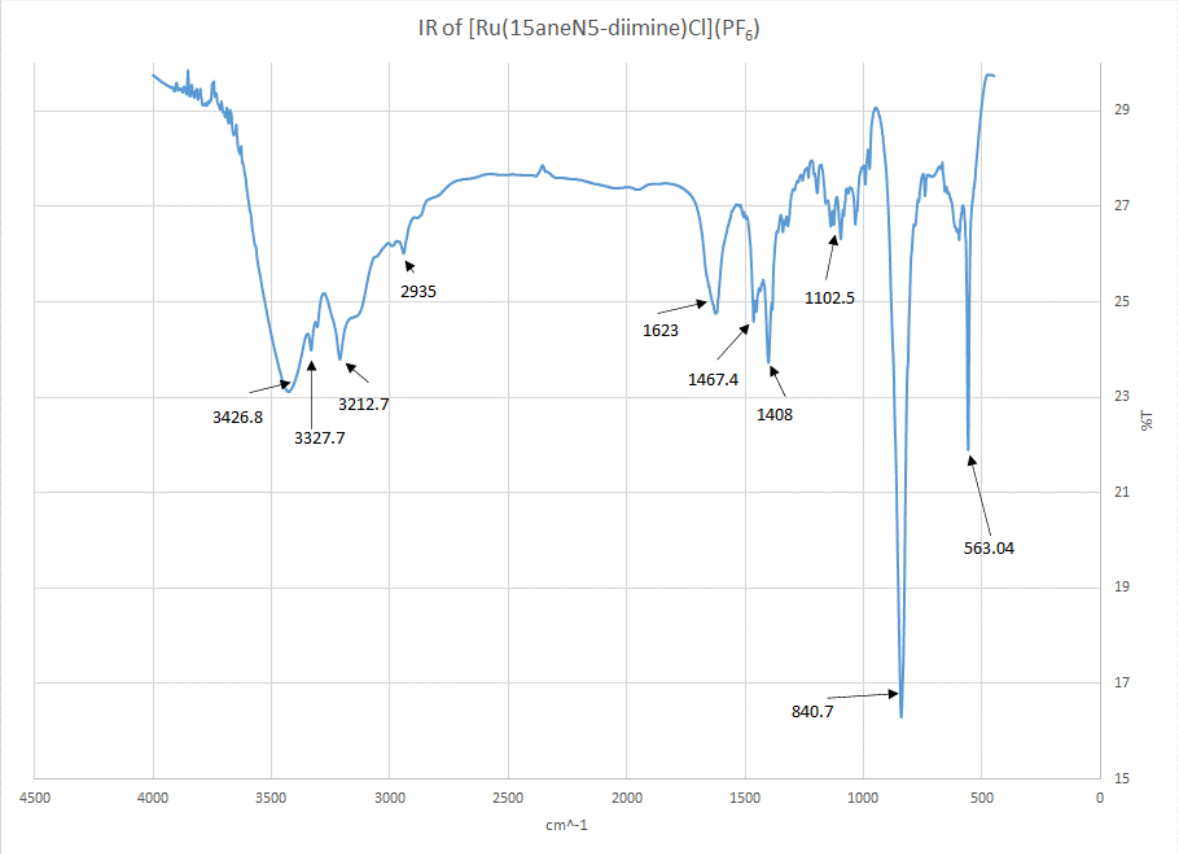

Figure S15: IR in KBr Pellet of MG07B, [Ru(**15aneN5-diimine**)Cl](PF$_6$)

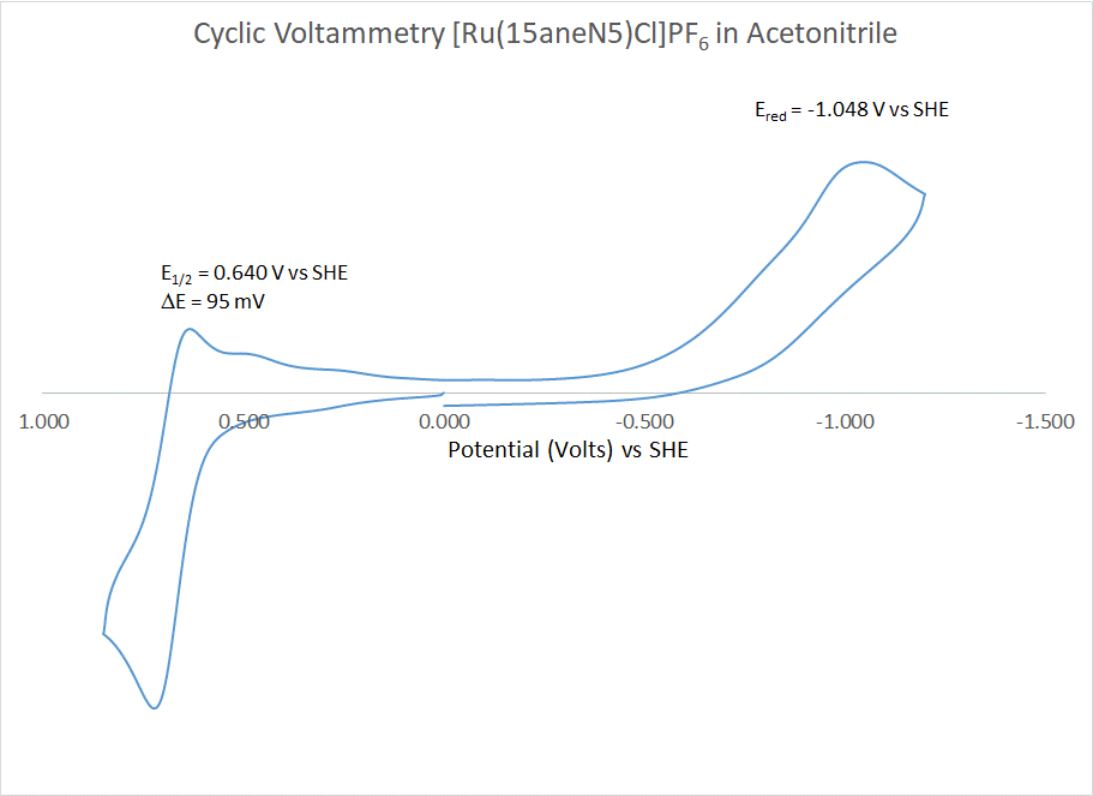

Figure S16: Cyclic Voltammogram in Acetonitrile of MG07B, [Ru(**15aneN5-diimine**)Cl](PF$_6$)

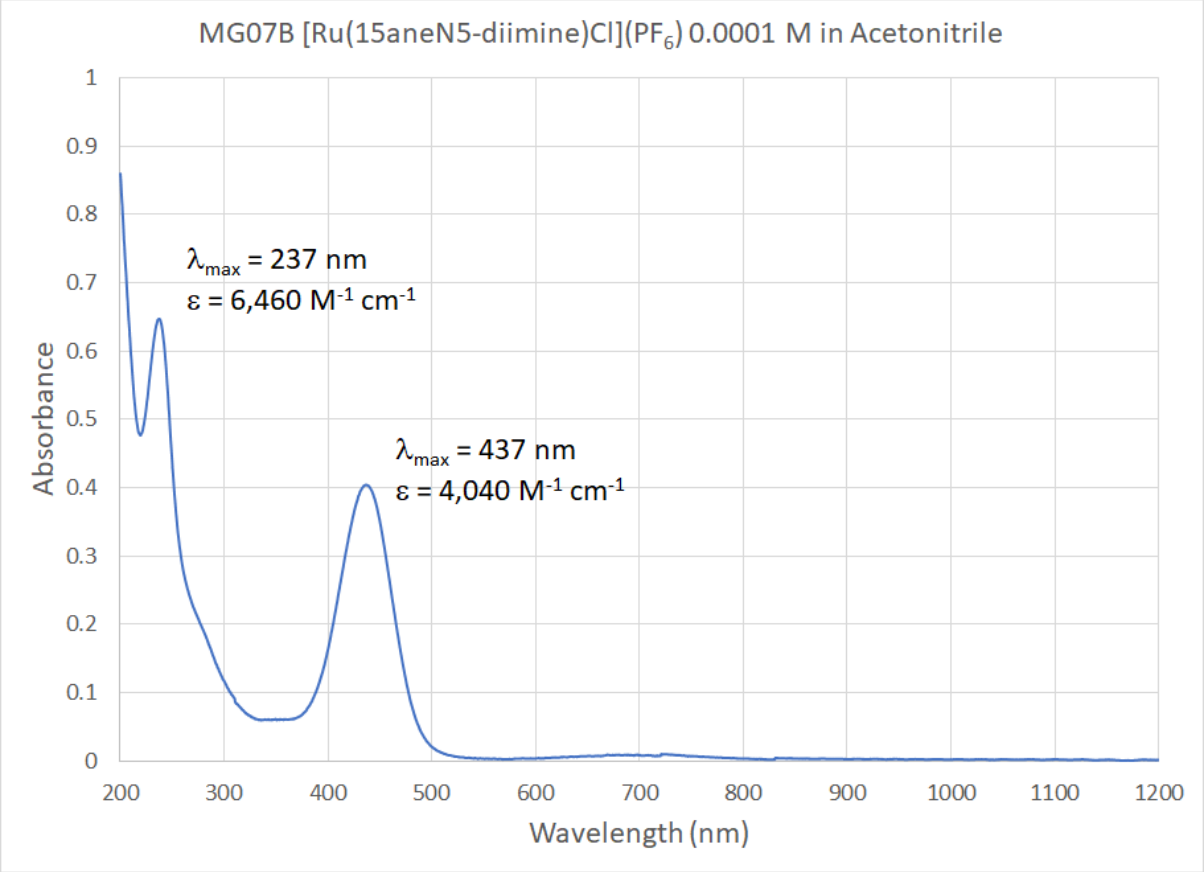

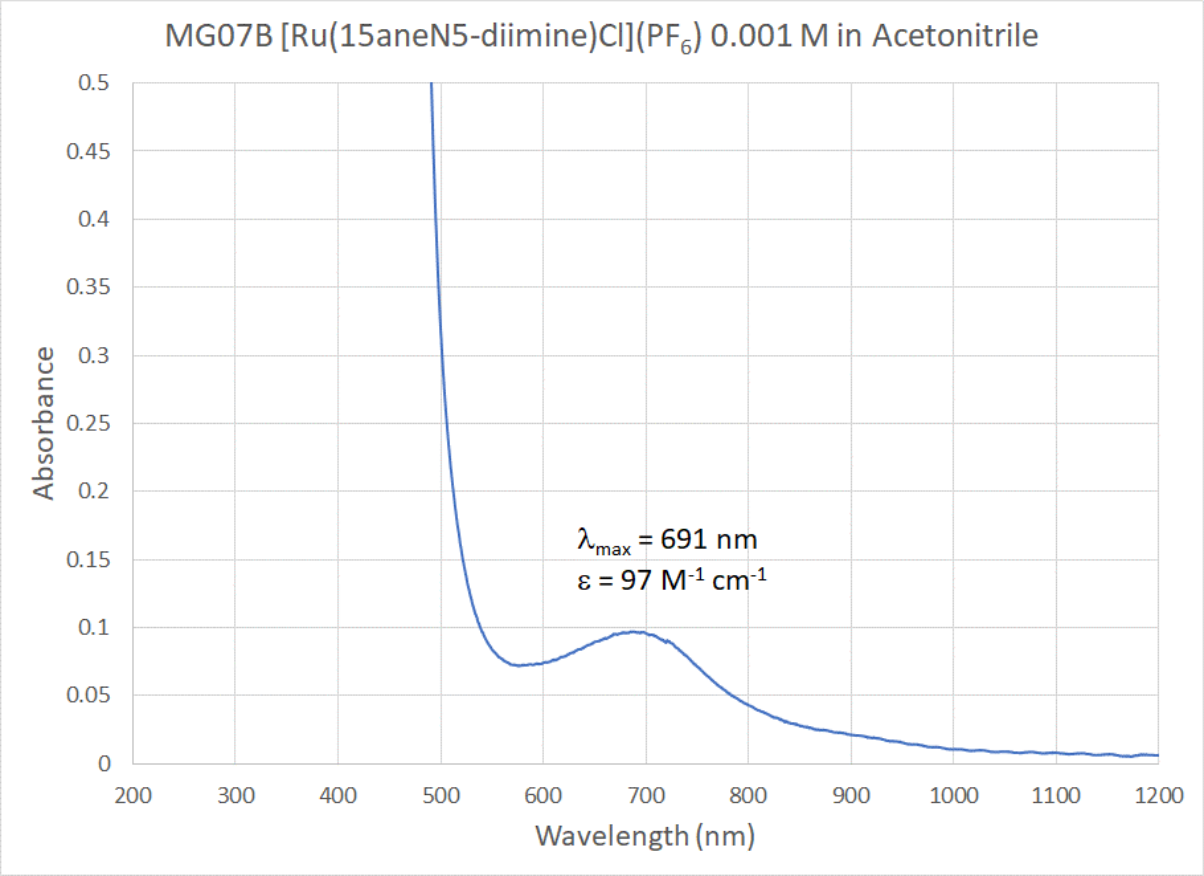

Figure S17: UV-Vis Spectra in Acetonitrile of MG07B, [Ru(**15aneN5-diimine**)Cl](PF_6)